

Review

# Progress in Solid Oxide Fuel Cells with Hydrocarbon Fuels

Mohamad Fairus Rabuni <sup>1,\*</sup> , Tao Li <sup>2,\*</sup>, Mohd Hafiz Dzarfan Othman <sup>3</sup>, Faidzul Hakim Adnan <sup>1</sup> and Kang Li <sup>4,\*</sup>

<sup>1</sup> Sustainable Process Engineering Centre (SPEC), Department of Chemical Engineering, Faculty of Engineering, Universiti Malaya, Kuala Lumpur 50603, Malaysia; faidzulhakim.adnan@um.edu.my

<sup>2</sup> MOE Key Laboratory of Energy Thermal Conversion & Control, School of Energy and Environment, Southeast University, Nanjing 211189, China

<sup>3</sup> Advanced Membrane Technology Research Centre (AMTEC), Faculty of Chemical and Energy Engineering, Universiti Teknologi Malaysia (UTM), Skudai, Johor Bahru 81310, Malaysia; dzarfan@utm.my

<sup>4</sup> Barrer Centre, Department of Chemical Engineering, Imperial College London, Exhibition Road, London SW7 2AZ, UK

\* Correspondence: fairus.rabuni@um.edu.my (M.F.R.); 101012902@seu.edu.cn (T.L.); kang.li@imperial.ac.uk (K.L.)

**Abstract:** Solid oxide fuel cells (SOFCs)' main advantage in fuel flexibility appears to be an interesting subject for further exploration. From the literature survey, direct utilisation of hydrocarbon as fuel for SOFCs has garnered attention with promising results reported. Various approaches, showcasing potential for using methane (CH<sub>4</sub>) and heavier hydrocarbons in SOFCs, have been described. The direct use of hydrocarbons can occur through either direct internal reforming or gradual internal reforming, with requisite precautionary measures to mitigate carbon formation. While the internal reforming process could proceed via steam reforming, dry reforming or partial oxidation, an exciting development in the direct use of pure hydrocarbons, seems to progress well. Further exploration aims to refine strategies, enhance efficiency and ensure the long-term stability and performance of hydrocarbon-fuelled SOFC systems. This review delves into the progress in this field, primarily over the past two decades, offering comprehensive insights. Regardless of fuel type, studies have largely concentrated on catalyst compositions, modifications and reaction conditions to achieve better conversion and selectivity. Finding suitable anode materials exhibiting excellent performance and robustness under demanding operating conditions, remains a hurdle. Alternatively, ongoing efforts are directed towards lowering working temperatures, enabling consideration of a wider range of materials with improved electrochemical performance.

**Keywords:** SOFC; hydrocarbons; direct utilisation; fuel flexibility



**Citation:** Rabuni, M.F.; Li, T.;

Othman, M.H.D.; Adnan, F.H.; Li, K.

Progress in Solid Oxide Fuel Cells

with Hydrocarbon Fuels. *Energies*

2023, 16, 6404. [https://doi.org/](https://doi.org/10.3390/en16176404)

10.3390/en16176404

Academic Editor: Jin-Soo Park

Received: 30 July 2023

Revised: 25 August 2023

Accepted: 2 September 2023

Published: 4 September 2023



**Copyright:** © 2023 by the authors.

Licensee MDPI, Basel, Switzerland.

This article is an open access article

distributed under the terms and

conditions of the Creative Commons

Attribution (CC BY) license ([https://creativecommons.org/licenses/by/](https://creativecommons.org/licenses/by/4.0/)

[https://creativecommons.org/licenses/by/](https://creativecommons.org/licenses/by/4.0/)

4.0/).

## 1. Introduction

In recent years, interest has increased in developing a highly efficient, low-carbon and renewable energy conversion system, as greenhouse gases release from the conventional energy generation methods have become widely known to be harmful to the environment. The most common combustion of fossil fuels has long been used for energy generation, although it suffers from relatively low efficiency and contributes to environmental pollution. Thus, a more efficient and environmentally benign technique to produce energy is required. Fuel cell technology is an encouraging technique to generate energy by directly converting the chemical energy in fuel into electricity through electrochemical reaction. It is a practical application, promising a better, clean alternative source of energy. There are various types of fuel cells that can be characterised according to their particular materials, the charge being transported, their electrolyte and operating temperature. The reader is referred to several review papers for a more thorough description [1–9]. Among all types of fuel cell, solid oxide fuel cells (SOFCs) have attracted considerable attention because of two remarkable features related to their high operating temperature. First, it provides fuel flexibility, allowing the use of hydrocarbons, syngas and biofuels. Secondly, SOFCs generate a

considerable amount of exhaust heat that may be used in combined heat and power systems (CHP) for even higher efficiency. Additionally, a major difference between an SOFC and its counterparts is the use of solid-state electrolyte. Its application can bypass common issues encountered with liquid electrolyte such as corrosion and electrode wetting [10]. SOFCs are also renowned for low emission of pollutants owing to their high conversion efficiency and could offer a quiet performance, since no moving parts or vibration are involved.

To date, several review papers are available in the literature with regards to the development of the SOFC anode materials and challenges for further development. For instance, McIntosh and Gorte have reviewed the progress of anode materials for SOFCs operating with hydrocarbons [11]. Sun and Stimming have also described and summarised various types of anode materials for hydrocarbon-fuelled SOFCs, the development of anode kinetics and reaction mechanisms, as well as the anode models and the economical processing methods for making anode [12]. Shi et al. have discussed the anodic reactions in hydrocarbon-fuelled SOFCs and strategies to improve anode performance and stability [13]. Shabri et al., on the other hand, have described the recent progress in the hydrocarbon-fuelled SOFC system which focused on the development of a metal–ceramic anode [14]. Their review highlighted the anode fabrication using either metal or metal alloy as cermet following the metal oxide reduction via hydrogen (H<sub>2</sub>) route. They presented a comprehensive discussion on the exploration of core components of the SOFC and delved into the most harmful degradation mechanisms they encountered, addressing poisoning, microstructural deformations and strains during operation [10]. More recent reviews on the progress in low-temperature (LT)-SOFC, highlighting the use of proton-conducting SOFCs with hydrocarbon fuels have been provided by Su and Hu [8] and Liu and Duan [9].

Worldwide interest in SOFCs has dramatically increased over the past decades as indicated by the tremendous growth in the number of patents applied as well as publications. Various leading institutions such as Colorado School of Mines, USA, University of Pennsylvania, USA, National Institute of Advanced Industrial Science and Technology (AIST), Japan, the University of St. Andrews, UK, are among those actively involved in this research field, as can be seen in Figure 1, which is the output of the result analysis using Scopus with keywords “hydrocarbon” and “solid oxide fuel cell” from year 1970 up until 2023. Nonetheless, several concerns regarding SOFC operation with hydrocarbons remain the focus of ongoing research quests. These include the rate-limiting electrochemical steps on anode, the nature of hydrocarbon reactions, the mechanisms for coking as well as the appropriate operating conditions by which stable coke-free operation can be maintained.

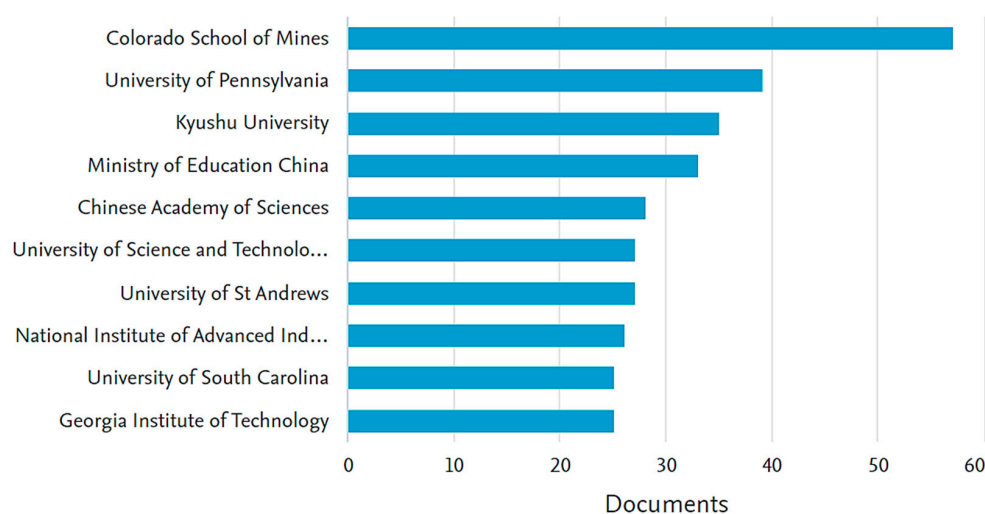


**Figure 1.** Number of documents/publications from various leading institutions worldwide related to hydrocarbon–solid oxide fuel cell.

In this review, we present the progress in hydrocarbon-fuelled SOFCs, particularly those featuring Nickel (Ni)-based anodes and oxide-ion-conducting electrolyte by examining the research output on this subject primarily from the past 20 years. The following section covers inclusive information on different approaches available for direct utilisation of hydrocarbons. Section 1 presents the background of the SOFCs operation with hydrocarbon fuels, while Sections 2 and 3 summarise information on an SOFC system operated by methane (CH<sub>4</sub>) and heavier hydrocarbons, respectively. As our emphasis is placed on the research with Ni-based anodes operated by hydrocarbons, therefore Sections 2 and 3 largely report different existing strategies and results with respect to the electrochemical performance for works using Ni-based cells. Section 4 analyses the literature and tries to propose next research advances, mainly on the development of anode, stable operating conditions and microstructure tailoring of the cell. Ultimately, a sound understanding of the various approaches to hydrocarbon-fuelled SOFCs is crucial for better improvement and optimisation, aiming at accelerating the commercialisation of an SOFC system for a variety of applications.

### *1.1. Comparison between Oxide-Ion-Conducting SOFCs and Proton-Conducting SOFCs Fuelled by Hydrocarbons*

Both oxide-conducting and proton-conducting SOFCs present distinct advantages and challenges when using hydrocarbon fuels. Generally, oxide-conducting SOFCs demonstrate superior efficiency due to their elevated operating temperatures and swift oxide ions transport [14]. This leads to improved energy conversion from hydrocarbon fuels, enhancing overall performance. By contrast, although proton-conducting SOFCs operate at lower temperatures where it provides the advantages in material stability and longevity [15], a trade-off arises in terms of efficiency compared to oxide-conducting SOFCs. In addition, oxide-conducting SOFCs prove more adept at accommodating a broad spectrum of hydrocarbon fuels, affording greater fuel flexibility, courtesy of their high operating temperature that facilitates efficient fuel reforming. On the contrary, proton-conducting SOFCs may necessitate specific reforming conditions to attain optimal performance. Additionally, both types of SOFCs face material selection challenges. Oxide-conducting SOFCs require materials capable of enduring high temperatures, potentially impacting long-term stability. In contrast, proton-conducting SOFCs benefit from lower operating temperatures yet encounter challenges linked to proton conductivity and slower kinetics.

Oxide-conducting SOFCs are typically more resilient against carbon formation when supplied with hydrocarbon fuels. Their higher operating temperatures and thermodynamic conditions enable efficient carbon management, reducing the risk of carbon deposition and ensuring prolonged cell performance. This distinction highlights the importance of considering the type of SOFC electrolyte when utilising hydrocarbon fuel to achieve clean and efficient energy conversion. When considering the use of hydrocarbons, oxide-conducting SOFCs appear as a compelling choice given by their higher efficiency, greater fuel flexibility and resistance to carbon deposition. These attributes align remarkably well with the imperatives of efficient energy conversion and sustainable use of hydrocarbon feedstocks. While proton-conducting SOFCs offer advantages in certain contexts, such as lower operating temperatures, their limitations in terms of efficiency and carbon management underscore the significance of oxide-conducting SOFCs for effectively harnessing the potential of hydrocarbon fuels in clean energy applications [16]. In addition, the materials employed in the fabrication of proton-conducting SOFCs are comparatively more expensive than those used for oxide-conducting SOFCs.

Recent work by Mojaver et al. entailed the simulation of a power generation system that utilizes an integrated CH<sub>4</sub>-fed SOFC and organic Rankine cycle (ORC), with validation carried out using available experimental data [17]. The model underwent thorough validation against the literature data. A comprehensive comparative assessment of the system's performance was then undertaken, comparing the oxide-conducting SOFC with the proton-conducting SOFC. This analysis encompassed evaluations across energy, exergy,

economic and environmental perspectives. The input variables taken into account were the current density and stack temperature. The findings pointed to the superiority of the oxide-conducting SOFC across various domains, i.e., energy, exergy, economic and environmental, when operating under their respective optimal conditions. It is noteworthy that this deduction is likely to hold consistently within the explored ranges of decision variables.

As the global energy landscape continues to progress, the better performance of oxide-conducting SOFCs with hydrocarbon fuels positions them as a frontrunner in the pursuit of a cleaner and more sustainable energy future.

### 1.2. Mode of Operations for Hydrocarbon SOFCs

The use of hydrocarbons from fossil fuel or renewable sources is desirable for energy generation as certain difficulties associated with hydrogen ( $H_2$ ) production, safety, storage and distribution have yet to be resolved [18–20]. With escalating demand and limited supply, hydrocarbons will become even more pricey, emphasising the importance of high conversion efficiency of energy generation devices such as SOFCs. While significant progress has been achieved in  $H_2$ -fuelled SOFC studies, investigations continue into the potential use of hydrocarbons. Fuel flexibility is one attractive feature of SOFCs, as they may operate using hydrocarbon fuels, i.e., natural gas, biogas, etc., with less fuel processing compared to other fuel cell types [21].

For hydrocarbon-fuelled oxide ion-conducting SOFCs, there are several modes of operations including external fuel reforming prior entering the cell, internal reforming or directly feeding the pure hydrocarbon into the cell [22]. These approaches are represented in Figure 2, where Figure 2a shows the ideal operation with direct oxidation of the hydrocarbon fuels, and Figure 2b–d illustrate the reforming of hydrocarbon fuels either through external reforming, indirect internal reforming or direct internal reforming, respectively.

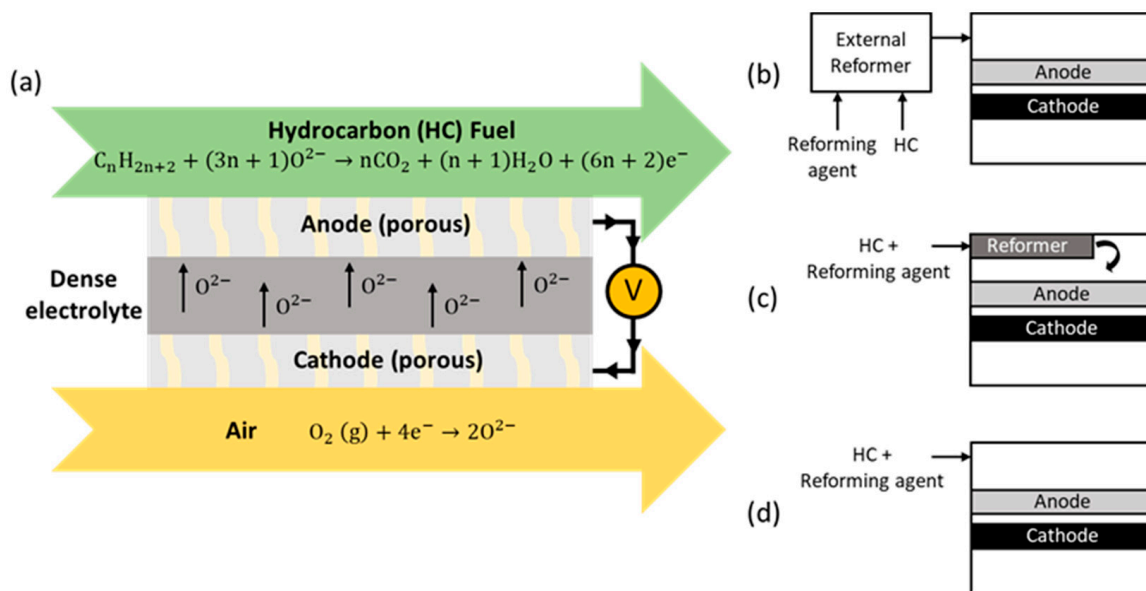


**Figure 2.** Hydrocarbon-fuelled SOFCs with oxide-conducting electrolyte through (a) direct oxidation of the hydrocarbon fuel, (b) external reforming, (c) indirect internal reforming and (d) direct internal reforming.

The reforming process transforms the hydrocarbon to simpler fuels, i.e.,  $H_2$  and  $CO$ , which can then be used directly in a fuel cell. While  $CO$  may be considered as a contaminant in most low-temperature fuel, SOFCs can be operated by it. This helps to simplify the fuel process by excluding the purification step. Fuel reforming can be performed externally, using a separate fuel processor known as a reformer, or internally at the anode (Figure 2b). A variant of internal reforming is either to add a separate reforming catalyst within the

anode compartment (indirect internal reforming represented by Figure 2c) or directly on the anode (direct internal reforming as shown in Figure 2d) [23]. In a system with indirect internal reforming, reforming catalyst was integrated within the SOFC at the entry point of the hydrocarbons in anodic compartment. However, there could be a significant gradient between the rates of endothermic and exothermic reactions. This would cause a consequential decrease in local temperature at the upstream of anodic compartment that could lead to mechanical failure resulting from thermally induced stresses [24]. Alternatively, direct internal reforming works by the principle of direct feed of SOFCs using a mixture of fuel and reforming agents. This mode in overall offers lower operational cost, reduces the system complexity and necessitates less maintenance thanks to the relinquishment of external reformer, making the system more desirable.

Another considerable interest has been given to a process whereby hydrocarbon-rich fuel is directly fed into the anode compartment (i.e., without the reforming agents). Since external reforming increases complexity and cost to the system, direct feed of hydrocarbon-rich fuel offers substantial advantages. This approach is poised to attain higher energy conversion efficiency in addition to the least fuel processing of the system. The direct use of hydrocarbons for SOFCs is, in principle, possible and attractive thanks to the particular prospect of gradual internal reforming of hydrocarbons. Conditionally, the anode material needs to satisfy several ideal criteria, including high catalytic activity for fuel oxidation and excellent ionic and electronic conductivity. At high SOFC working temperatures, either the direct electrochemical oxidation or the internal reforming/partial oxidation of the hydrocarbons becomes kinetically favourable. Nevertheless, these different modes of operation mentioned above have both advantages and disadvantages. Research into each method is still continuing to gain further understanding of the reaction mechanism, better cell performance and eventually helps to accelerate commercialisation. Overall, a different approach when dealing with an SOFC with Ni-based anode when operated with hydrocarbon fuels must be carefully considered with the major aim to avoid carbon formation to ensure stable performance.

### 1.3. Direct Hydrocarbon Utilisation

In theory, the use of hydrocarbons directly may improve the overall efficiency of a system. It is, however, worth mentioning that the understanding of “direct use of hydrocarbon fuels” by electrochemical means is still ambiguous. Compared to the well-understood chemical oxidation of hydrocarbons (i.e., hydrogenation and hydrogenolysis, partial oxidation and complete oxidation), the electrochemical oxidation of hydrocarbons is less well understood. In the literature, several terms have been introduced to designate “direct use of hydrocarbon fuels” such as direct utilisation, direct conversion or direct oxidation. This might lead to confusion and misinterpretation of precise definitions.

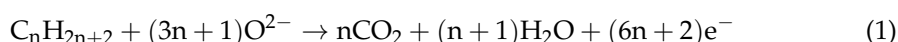
Mogensen and Kammer defined direct conversion of a hydrocarbon during SOFC operation as the “conversion in the SOFC without pre-mixing the fuel gas with steam or carbon dioxide (CO<sub>2</sub>) and without processing the fuel before it enters the cell stack” [19]. This implies that the reaction is either through direct electrochemical oxidation or electrochemical oxidation of cracking products with the open circuit voltage (OCV) equals to the Nernst potential. Thus, all steps in the reaction of hydrocarbon conversion must be electrochemical in nature and any reaction pathways that encompass hydrocarbon cracking and electrochemical oxidation of the cracked products are not considered as direct oxidation. In our view, to interpret “direct use of hydrocarbon fuels” to be equivalent to “direct oxidation” is fairly rigid and unfeasible for actual application and, thus, less suitable.

Besides, it has been described that the direct electrochemical oxidation of hydrocarbons is unlikely to occur in one step [25,26]. Gas chromatography (GC) analysis has shown that partial oxidation reactions are dominant for some oxide anodes [27]. For that reason, to define “direct use of hydrocarbons” to be similar to “direct oxidation” seems impractical. McIntosh and Gorte instead suggested a broader definition describing the direct use of hydrocarbon fuels in an SOFC using the term “direct hydrocarbon utilisation” [20]. By this



meaning, besides a process wherein a dry (i.e., pure) fuel is fed into the system, it also takes in humidified fuels (approximately 3 vol.% H<sub>2</sub>O), regardless of the exact reaction steps [20]. For practical reasons, such a definition is used throughout this review.

It is expected that operations with hydrocarbons as fuel will be much more complex than those using the simpler operating principle of a H<sub>2</sub>-fuelled system. As shown in Figure 3, there is a possibility of different parallel pathways during direct hydrocarbon use in SOFC, each with various individual steps. The ideal reaction for a hydrocarbon-fuelled SOFC is direct oxidation (Figure 2a), in which oxide ions (O<sup>2-</sup>) from the cathode travel through the electrolyte and oxidise the hydrocarbon at the anode triple phase boundary (TPB), a region at which the three components, oxygen ions, electrons and fuels, meet. This ideal and straightforward reaction represented by the following equation releases the most energy since no endothermic processes are involved:



However, this requires effective catalysts and careful control of operating conditions. It may also involve multiple steps, along with side reactions such as pyrolysis and oligomerisation. Since side reactions are inherent during the actual operation, the electrochemical reactions for hydrocarbon fuel may proceed either through (1) oxidation of cracked carbon and hydrogen, (2) oxidation of an oxygenated compound or (3) oxidation of the intermediates produced from free radical reactions.

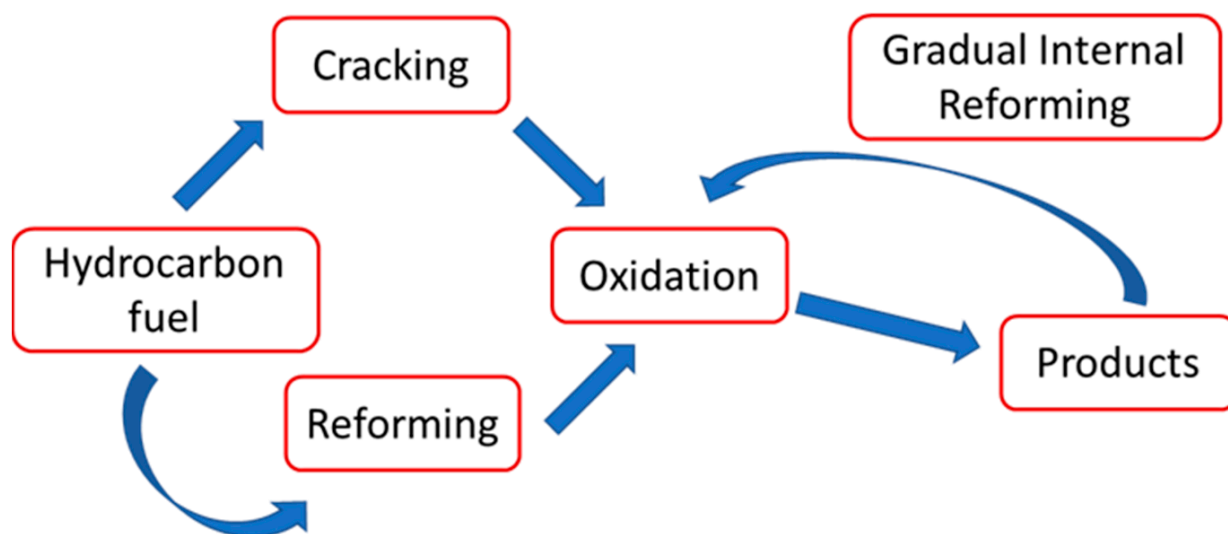


Figure 3. Different paths for hydrocarbon utilisation in the SOFC system.

Although an SOFC offers the advantage of fuel flexibility, its choice is still limited by the affinity of the hydrocarbons to foul the regularly used Ni–cermet anode surface. This fouling which is caused by the carbon formation has become a major impediment that needs to be solved for stable SOFC operation. Unless a suitable catalyst is present to realise direct oxidation of hydrocarbons to minimise this problem, hydrocarbons must be reformed prior to the electrochemical reactions. Another concern is catalyst poisoning by contaminants such as hydrogen sulphide (H<sub>2</sub>S), which could poison the catalyst containing anodes. There have been several comprehensive reviews about this topic [28,29], where interested readers can refer to and it is worth mentioning that it is beyond the scope of this review.

#### 1.4. Carbon Formation

An intrinsic problem in SOFC operation when using hydrocarbons as fuel is the formation of carbon through undesired side reactions. It has been reported that the deposition of carbon disrupts the performance of an SOFC, particularly one with Ni-based anodes, as Ni itself is an excellent catalyst for C-C and C-H bond breakage [30]. At high temperatures, hydrocarbon reactions may occur not only on the anode surfaces but also at the interconnect plates and the tubes connecting to the anode compartment. It could also happen in the gas phase via free-radical cracking and polymerisation, forming tar. This deposited carbon can cause pore blockage, obstruct reforming reactions through catalyst particle encapsulation and increase transport resistance to gases trying to reach the TPB, hence lowering the overall system performance.

If this technology is to be practical and economical, understanding the mechanism of carbon formation is indispensable. There are two mechanisms that have been generally reported: first, heterogeneous reaction on catalyst surfaces, producing carbon nanowires or nanofibres, and secondly, homogeneous reaction in the gas phase, forming soot capable of being ubiquitously deposited at the anode. This soot or pyrolytic carbon may cover and deactivate the catalyst. Thorough explanations of these mechanisms have been given by other researchers [19,20,22,31].

There are several factors that affect the degree of carbon formation including reforming agent to carbon (i.e., steam/C or  $\text{CO}_2/\text{C}$ ) ratio, operating conditions and catalyst material. Keeping the fuel within an equilibrium noncoking condition is one way for maintaining stable coke-free operation [20]. This region of stability for hydrocarbon fuels could be mapped based on thermodynamic calculations and would be a useful reference for avoiding severe effects of carbon deposition. Accordingly, selecting appropriate operating conditions (e.g., temperature, pressure and current density) may minimise the severity of the problem, if not totally eliminate it. As can be seen in Figure 4, the composition triangle for C-O-H shows carbon formation limits at 1000 °C, while 800 °C is close to 1:1 for a C/O ratio but displays a considerable discrepancy at a lower temperature. The addition of an ample amount of reforming agent ( $\text{H}_2\text{O}$ ,  $\text{CO}_2$  or  $\text{O}_2$ ) aids in diminishing the formation of carbon.

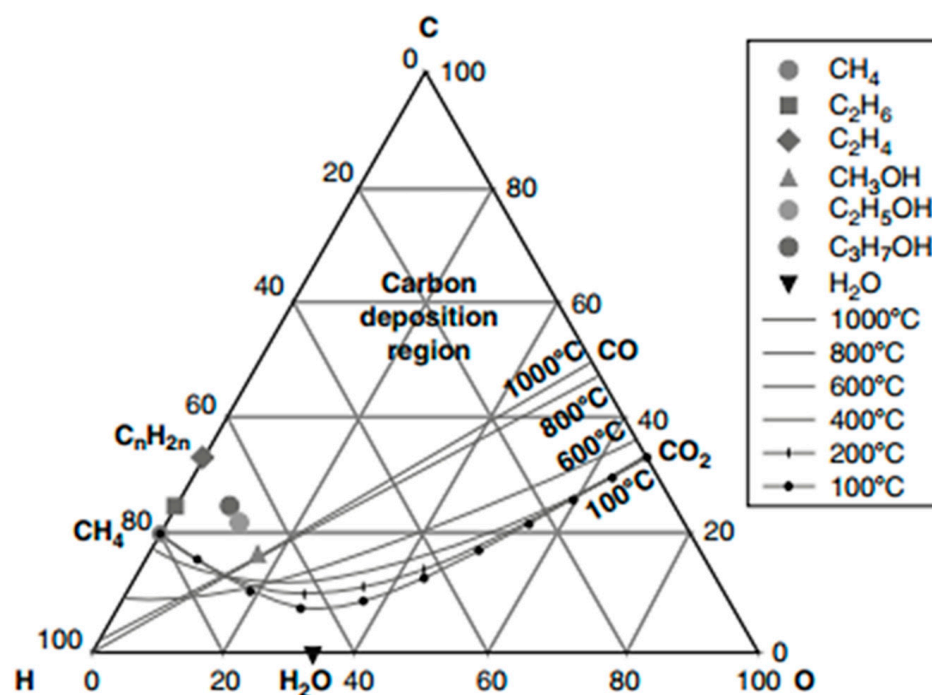


**Figure 4.** Carbon deposition limit boundaries for a C-H-O composition for various types of hydrocarbons. Figure is adapted from [32].

Appropriate choice of catalytic material for reforming steps is another important issue to ensure stable system performance. The material has a substantial role as it must be efficient in preventing carbon formation and steady for long-term usage while remaining cost-effective. It is also worth mentioning that several studies reported that the actual ratio of reforming agent to carbon for efficiently suppressing coke formation considerably differs from that expected by thermodynamic calculations. This large discrepancy can be associated with the fact that thermodynamic calculations only provide insight into the predicted equilibrium conditions and do not consider the influence of reaction kinetics [33]. In this light, numerous researchers have examined the reaction kinetics of carbon formation, in search of optimum operating conditions and better materials for the anode [34].

Despite the challenges regarding carbon formation, direct hydrocarbon-fuelled SOFCs are interesting in terms of simplification of fuel processing and the overall energy costs may be substantially reduced. Works on this operation mode have been actively researched for the past two decades, whereby several approaches, including internal reforming or even direct feeding of the fuel into the cell have been studied. There does exist a major difference between the operation with methane ( $\text{CH}_4$ ) and other higher molecular weight hydrocarbons (heavier hydrocarbons) as fuel. Theoretically, the molecule of  $\text{CH}_4$  is simpler and relatively more stable and thus could be used directly (in undiluted form) with less tendency towards coking. Heavier hydrocarbons (i.e., other than methane), on the contrary, incline to cause a considerable coke or tar deposition on the anode or fuel-compartment surfaces, even when mixed with steam (steam reforming) or carbon dioxide (dry reforming). Therefore, the strategy to deal with heavier hydrocarbons may be differ from that of  $\text{CH}_4$ -fuelled system. These processes are further elaborated upon in subsequent sections.

## 2. Methane-Fuelled SOFCs

Methane ( $\text{CH}_4$ ), as an abundant resource and the main element of natural gas, is predicted to become the major hydrocarbon feedstock in future [35]. Natural gas is a fossil fuel that is much cleaner than coal and oil due to its higher hydrogen (H) to carbon (C) ratios in its molecular composition and contains a trivial amount of nitrogen (N) and sulphur (S) impurities. Other than that,  $\text{CH}_4$  is also the main constituent in biogas with CO as the remainder. The biogas is produced from anaerobic fermentation of various organic matters such as manure, wastewater sludge, municipal solid waste or another decomposable feedstock. Accordingly,  $\text{CH}_4$  could be viewed as a promising renewable energy resource which is important for energy generation.

To date, most studies conducted on hydrocarbon utilisation in SOFCs have used  $\text{CH}_4$  as fuel (Table 1). This is largely due to a chemical profile throughout its electrochemical process that is simpler than that of heavier hydrocarbons. Ni-cermets continue to be the most frequently applied materials for an SOFC anode. However, as previously described, they are prone to coking, restricting their use in hydrocarbon-fuelled system. As noted earlier, this review emphasis on the research of SOFCs with Ni-based anodes fuelled by hydrocarbons. Further modifications on the Ni-cermets properties are essential along with several other strategies have been proposed in the literature to resolve such issues. Various ways to use  $\text{CH}_4$  as fuel are discussed in the following sections which includes internal reforming mode either by steam,  $\text{CO}_2$  or partial oxidation, as well as direct utilisation. Table 1 lists the methane-fuelled SOFCs, mainly those with Ni-based anodes and oxide-ion-conducting electrolyte.



**Table 1.** Research progress in methane-fuelled SOFCs topic.

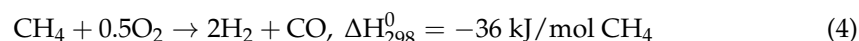
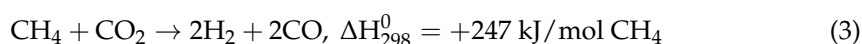
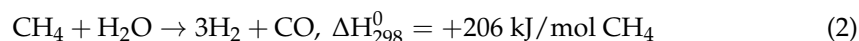
Anode	Electrolyte	Cathode	Fuel Stream	Temp. (°C)	OCV (V)	P <sub>max</sub> (W·cm <sup>-2</sup> )	Ref.
Ni-YSZ/YDC	YSZ	LSM	Wet CH <sub>4</sub> (3% H <sub>2</sub> O)	650		0.37	[36]
				600		0.25	
				550		0.125	
Ru-Ni-GDC	GDC	SDC	Dry CH <sub>4</sub>	600	~0.9	0.75	[37]
NiO-YSZ	YSZ	LSM	H <sub>2</sub> /CH <sub>4</sub>	850	1.0	/	[38]
Cu-Ni-CeO <sub>2</sub> -YSZ	YSZ	LSM	Dry CH <sub>4</sub>	800	1.0	0.33	[39]
Ni-Cu-CeO <sub>2</sub> -YSZ	YSZ	LSM	H <sub>2</sub> /CH <sub>4</sub> /C <sub>4</sub> H <sub>10</sub>	700	1.0	0.14	[40]
Ni-GDC-Ru	GDC	SSC	Dry CH <sub>4</sub>	600	0.9	0.75	[41]
Ni-YSZ	YSZ	LSM-YSZ	Wet CH <sub>4</sub> (3% H <sub>2</sub> O)	800	~1.17	0.96	[42]
Ni-YSZ	YSZ	LSCF-GDC	Wet CH <sub>4</sub> (3% H <sub>2</sub> O)	700	~1.2	0.52	[43]
				800		1.27	
Ni-YSZ	YSZ	LSCF-SDC	Dry CH <sub>4</sub>	800	~1.1	0.35	[44]
NiO-SDC	SDC	SSC	CH <sub>4</sub>	600	0.857	0.353	[45]
Ni-SDC	SDC (~20 μm)	SDC-BSCF	18.8% CH <sub>4</sub> + 16.2% O <sub>2</sub> + 65% He (by vol.)	787		0.76	[46]
Ni-YSZ	YSZ (~1 mm)	LSM	Dry CH <sub>4</sub>	900	0.55	~0.055	[47]
Ni-YSZ	YSZ	LSM	CH <sub>4</sub>	750	1.05	0.122	[48]
Ni-YSZ	YSZ	LSM	CH <sub>4</sub>	750	0.92	0.036	[49]
Ni-GDC Ni <sub>0.9</sub> Fe <sub>0.1</sub> -GDC	GDC	LSCF-GDC	Dry CH <sub>4</sub>	650	~0.8–0.82	0.30 0.34	[50]
Ni-YSZ	YSZ	LSCF-GDC LSCF-GDC-Ag (10 wt%)	CH <sub>4</sub> /air mixture of 25/60 mL min <sup>-1</sup>	700	~0.9 ~1.0	0.06	[51]
						0.12	
Ni-GDC	GDC	LSCF-GDC	CH <sub>4</sub> :H <sub>2</sub> O:N <sub>2</sub> 15:60:25 (i.e., S/C = 4)	550	0.85	0.45	[52]
Ni-GDC	GDC	LSCF-GDC	CH <sub>4</sub> /H <sub>2</sub> /H <sub>2</sub> O with a S/C = 2–3	550	0.72–0.78	~0.62	[53]
Ni-YSZ	YSZ-SDC (5 μm–5 μm)	BSCF-SDC	CH <sub>4</sub> -O <sub>2</sub> (2:1)	700	1.07	1.5	[54]
Ni-GDC	YSZ/GDC	LSCF	CH <sub>4</sub> /H <sub>2</sub> O S/C ratio = 0.079	610	1.08	0.26	[55]
NiO-YSZ	YSZ	/	Dry CH <sub>4</sub>	850	1.2	0.566	[56]
Ni-GDC Sn/Ni-GDC	GDC	LSCF	CH <sub>4</sub>	650	0.74–0.76	~0.37	[57]
						~0.47	
Ni-YSZ-BCZYb	YSZ (3 μm)	LSCF-GDC with a GDC buffer layer	36% CH <sub>4</sub> + 36% CO <sub>2</sub> + 20% H <sub>2</sub> O + 4% H <sub>2</sub> + 4% CO	750	~1.05	1.43	[58]
Li-Ni-SDC Na-Ni-SDC	LSGM (300 μm)	SCCO-SDC	Wet CH <sub>4</sub> (3% H <sub>2</sub> O)	800	1.13 1.02	0.212	[59]
						0.231	
NiO-YSZ	YSZ	LSCF	CH <sub>4</sub> :O <sub>2</sub> :N <sub>2</sub> (1:0.21:0.79) at 19% fuel utilisation rate at 38% fuel utilisation rate	650	at 0.7 at 0.7	~0.17	[60]
						~0.22	
LaNi <sub>0.6</sub> Co <sub>0.4</sub> O <sub>3</sub> -Ni- BZCYb	BZCYb (3 μm)	BZCY-LSCF	Wet CH <sub>4</sub>	650	~1.1	0.98	[61]
Ni-BZCYb-PBM-Ni- Co	BZCYb (~20 μm)	NBCaC-BZCYb	CH <sub>4</sub> -CO <sub>2</sub> (50:50%)	700	~1.0	1.25	[62]
Ni-LDC-Ni-SDC	SDC	SDC-BSCF	Wet CH <sub>4</sub>	650	~0.83	0.699	[63]
Ni-BZY	BZY	BCFZY0.1	CH <sub>4</sub> /C <sub>2</sub> H <sub>6</sub> /C <sub>3</sub> H <sub>8</sub> /N <sub>2</sub> 95/3/1/1% CH <sub>4</sub> (O:C = 2) CH <sub>4</sub> (O:C = 2.5)	600	~0.98 ~0.98 ~0.98	~0.37	[15]
				600		~0.36	
				600		~0.27	
NiO-YSZ	YSZ	GDC-LSCF	20% CH <sub>4</sub> –80% CO <sub>2</sub>	750	~0.96	2.2	[64]
Ni-BaO-CeO <sub>2</sub> @SiO <sub>2</sub> - NiO-YSZ	YSZ-SDC interlayer	BSCF-SDC	30% CH <sub>4</sub> –70% Air	800	~1.05	0.938	[65]

Ba<sub>0.5</sub>Sr<sub>0.5</sub>Co<sub>0.8</sub>Fe<sub>0.2</sub>O<sub>3-δ</sub> (BSCF); BaCo<sub>0.4</sub>Fe<sub>0.4</sub>Zr<sub>0.1</sub>Y<sub>0.1</sub>O<sub>3-δ</sub> (BCFZY0.1); BaZr<sub>0.1</sub>Ce<sub>0.7</sub>Y<sub>0.1</sub>Yb<sub>0.1</sub>O<sub>3-δ</sub> (BZCYb); La<sub>2</sub>Ce<sub>2</sub>O<sub>7</sub> (LDC); La<sub>0.8</sub>Sr<sub>0.2</sub>MnO<sub>3</sub> (LSM); La<sub>0.9</sub>Sr<sub>0.1</sub>Ga<sub>0.8</sub>Mg<sub>0.2</sub>O<sub>3-δ</sub> (LSGM); La<sub>0.6</sub>Sr<sub>0.4</sub>Co<sub>0.2</sub>Fe<sub>0.8</sub>O<sub>3-δ</sub>-Gd<sub>0.1</sub>Ce<sub>0.9</sub>O<sub>2</sub> (LSCF-GDC); Sr<sub>2</sub>MgMoO<sub>6-δ</sub> (SMMO); Sm<sub>0.5</sub>Sr<sub>0.5</sub>CoO<sub>3</sub> (SSC); Sr<sub>0.95</sub>Ce<sub>0.05</sub>CoO<sub>3-δ</sub> (SCCO); Ce<sub>0.8</sub>Sm<sub>0.2</sub>O<sub>2-x</sub> (SDC); NdBa<sub>0.75</sub>Ca<sub>0.25</sub>Co<sub>2</sub>O<sub>5+δ</sub> (NBCaC); (Y<sub>2</sub>O<sub>3</sub>)<sub>0.15</sub>(CeO<sub>2</sub>)<sub>0.85</sub> (YDC).

### 2.1. Internal Reforming

Thermodynamic means are one approach to controlling the formation of carbon during the operation of SOFCs with hydrocarbon fuels. This could be performed by introducing reforming agents such as steam or other oxygen-containing oxidants (CO<sub>2</sub> or O<sub>2</sub>) together with the fuels into the fuel cell system. The internal reforming is a straightforward process by simply mixing hydrocarbon with reforming agents at a certain ratio to transform into simpler fuels such as hydrogen (H<sub>2</sub>) and carbon monoxide (CO) in situ. Internal reforming of CH<sub>4</sub> and natural gas in SOFCs have been studied, either with or without partial pre-reforming [66,67]. However, operation with natural gas is slightly different from using pure CH<sub>4</sub> as some heavier hydrocarbons contained in the natural gas are likely to cause coking. Thus, the additional pre-reforming step is often required. An internal reforming process of pure CH<sub>4</sub>, instead, could be directly performed either through steam reforming, dry (CO<sub>2</sub>) reforming or partial oxidation. During SOFC operation, one major virtue is that heat is generated in the cell by electrochemical reactions, and this ohmic heating could be directly used for the endothermic reforming reaction [67].

Steam reforming, dry reforming and partial oxidation are expressed in Equations (2)–(4), respectively [68]. All of these reactions yield syngas with different CO/H<sub>2</sub> ratios: 1:1, 1:2 and 1:3 for dry, partial oxidation and steam reforming process, respectively.



where  $\Delta H_{298}^0$  is the reaction standard enthalpy at 298 K.

These different means for internal reforming are summarised in Table 2. Detailed information about these processes is discussed in the following sections.

**Table 2.** Description of different types of reforming process.

Reforming Process	Description
Steam reforming (SR)	A process in which high-temperature steam is added to hydrocarbons (fuel) that transform into simpler fuels: H <sub>2</sub> and CO.
Dry reforming (DR)	A process in which CO <sub>2</sub> acts as an oxidant in the presence of a suitable catalyst.
Partial oxidation (POx)	A chemical reaction between the hydrocarbons and oxygen (O <sub>2</sub> ) typically from the air in a substoichiometric ratio.

#### 2.1.1. Internal Steam Reforming

A study on SOFC operation with hydrocarbons with steam as an input has been conducted as early as in 1962 [69]. Reforming the fuel internally may help to diminish the energy required for water gasification and lead to process simplification as the external reformer can be excluded. It has been reported that the effectiveness of internal reforming to be greater than that of external reforming in the same SOFC system [70]. This process typically applies a steam-to-carbon (S/C) ratio of higher than two to suppress carbon deposition. More interestingly, in the presence of generated water from the electrochemical reaction at the anode, the reforming process could occur even at a lower S/C ratio. Therefore, the supply of CH<sub>4</sub> mixed with a small amount of steam directly to the system inlet is attractive for process simplification.

The operating temperature and S/C ratio have major influences on the degree of coke formation. A CH<sub>4</sub> internal reforming study using electrolyte-supported single cells with different types of anodes, i.e., Ni-YSZ and Ni-GDC (gadolinium-doped ceria), were performed at various S/C ratios, from 0 to 3 [71]. At 950 °C, virtually no discrepancy in the reforming activities of both anodes was observed. However, at a lower temperature of 800 °C, the conversion rate greatly relies on the anode material with a higher CH<sub>4</sub> conversion

obtained using a cell with Ni-GDC anode. A similar observation of catalytic activity for the reforming reactions has also been reported elsewhere [72]. It is often thought that a higher S/C ratio would lead to a more efficient reforming process as abundant steam would assist in gasifying deposited carbon and prevent carbon buildup. However, this may not always be the case, as a degradation of a Ni-YSZ anode has been discovered in a system operated with a S/C ratio of 3 [55]. The excess steam was found to oxidise nickel catalyst locally at a vicinity of the interface between electrolyte and anode. More important, excessive steam compromises power generation efficiency by diluting the fuel. Another drawback is that the endothermic nature of steam reforming reaction could cause local cooling where the resultant steep thermal gradient might mechanically damage the cell stack [73]. Although a lower S/C ratio is preferred, carbon may be formed at a ratio of less than one in the equilibrium causing poor electrochemical performance [74]. This is attributable to the deactivation of anode catalysts and the inhibition of fuel diffusion. Therefore, the S/C ratio should be carefully chosen depending on the type of anode materials and the operating conditions.

The improvement on the reforming process could be expected through the addition of catalytic materials into the Ni-based anodes. Incorporation of these catalysts as part of the anode may not only prohibit carbon deposition but also increase the electrochemical performance, as less water for reforming is needed. A noticeable reduction in carbon formation is observed on the modified Ni-YSZ cermets with small quantities (~1 wt%) of molybdenum (Mo) during CH<sub>4</sub> reforming, despite having a slight effect on the reforming activity and cell performance [73]. In contrast, another study employing a cell with copper (Cu)-based anodes reported an opposing outcome [75]. The deposition of MoO<sub>x</sub> has been believed to some extent to shield the electrocatalytic sites, reducing anode performance and thus being inappropriate in inhibiting coke formation. More research is, therefore, necessary to elucidate such discrepancies.

Takeguchi et al. performed a series of systematic studies on a modified Ni-YSZ anode for a system fuelled by CH<sub>4</sub> with a S/C ratio set at 2 [76,77]. Different alkaline earth oxides, such as calcium oxide (CaO), strontium oxide (SrO), ceria (CeO<sub>2</sub>) and magnesium oxide (MgO) have been incorporated to the conventional Ni-YSZ anodes [76]. With the first three oxides, carbon deposition was suppressed, while MgO incorporation increased the rate of carbon deposition and reduced the steam reforming activity. A high content of SrO (~2 wt%) in the anode, however, led to poorer CH<sub>4</sub> conversion. Further improvement in the reforming activity could be achieved with the addition of precious metals such as ruthenium (Ru) and platinum (Pt) that helps to increase the anode resistance towards coke formation [77]. In another work, CH<sub>4</sub> steam reforming was conducted on a cell with dual-layer anode, Ni<sub>0.5</sub>Cu<sub>0.5</sub>Fe<sub>2</sub>O<sub>4</sub> and Gd<sub>0.1</sub>Ce<sub>0.9</sub>O<sub>1.95-δ</sub> (NCF-GDC) composite, screen printed onto Ni-YSZ [78]. No significant signs of coking were detected during the operation using CH<sub>4</sub>-H<sub>2</sub>O (7 mol%) mixture as fuel at 800 °C and 0.20 A cm<sup>-2</sup>. On the contrary, poor electrochemical performance was observed with fuel mixture containing an excessive amount of steam (20 mol% H<sub>2</sub>O) corresponding to fuel dilution.

Aiming at lowering SOFC operating temperature to less than 600 °C, Suzuki and co-workers have introduced a functional layer made of pure ceria, placed on top of the conventional anode surface [52]. Such a layer was beneficial in improving the maximum power density to 0.45 W cm<sup>-2</sup> from 0.35 W cm<sup>-2</sup> for a cell without such a layer when operated at 554 °C fuelled with CH<sub>4</sub> and steam mixture with nitrogen (CH<sub>4</sub>/H<sub>2</sub>O/N<sub>2</sub> = 15/60/25 mL min<sup>-1</sup>). This additional layer allows reforming of CH<sub>4</sub> into H<sub>2</sub> and CO, which later being electrochemically oxidised within the anode–electrolyte TPB region.

Notwithstanding their practicality and effectiveness during SOFC operation, there are several concerns with regards to internal steam reforming that must be addressed. The endothermic nature of the process assists in cooling the stack, and it may be difficult to retain a uniform temperature and H<sub>2</sub> content throughout the stack. Severe cooling may take place near the fuel inlet if the reforming reaction is too rapid, causing a very large temperature gradient along the stack [67,79]. This shortcoming may give rise to inhomogeneous

geneous temperature distributions which is detrimental to the mechanical properties of the cermet anode. One potential solution is to ensure an optimal operation wherein the reforming reaction and the electrochemical reactions progress at similar rates [80].

### 2.1.2. Internal Dry Reforming

Steam can be replaced by carbon dioxide (CO<sub>2</sub>) as a reforming agent, a process known as dry reforming [81]. Other than being applied for producing synthesis gas (syngas) in the presence of a suitable catalyst, this technique appears to be a potential approach to mitigating greenhouse gases [82]. It is attractive from an industrial standpoint, as the resulting syngas has a low H<sub>2</sub> to CO ratio, suitable for Fischer–Tropsch reactions, a process to yield liquid hydrocarbons. This reforming system is also practical, given that both CH<sub>4</sub> and CO<sub>2</sub> are abundantly available and inexpensive. Despite its benefits, the reaction is very endothermic ( $\Delta H_{298}^0 = 247 \text{ kJ mol}^{-1}$ ), requiring an extensive amount of energy. Moreover, reforming catalysts, which are often Ni-based, are susceptible to deactivation due to coke deposition. Hence, these issues need to be first addressed, and one way of doing it is by developing catalysts that have excellent activity and high resistance against coking [35,83]. In addition to Ni-based catalysts [84,85], other types of catalysts have been explored for this reaction, such as with precious metals, e.g., iridium (Ir), Rh, Ru, Pd, Pt and others [86–88]. These materials were reported to have an encouraging catalytic performance with respect to activity and selectivity to syngas formation. Precious metals are renowned for their outstanding coking resistance, yet do not seem to be practical for large-scale uses for economic reasons.

Alternatively, ceria (CeO<sub>2</sub>) doped with materials such as zirconium (Zr), praseodymium (Pr) and niobium (Nb) were mixed with Ni and have been applied as anodes for an SOFC operated on CH<sub>4</sub>-CO<sub>2</sub> mixture [84]. The anodes were prepared by a hydrothermal method with a Ni content (14 vol.%), much lower than that of typical SOFC anodes (i.e., 30 vol.%). Among these, an anode containing Zr showed the lowest Ni crystallite size leading to a high initial activity on CH<sub>4</sub> dry reforming at 800 °C. Overall, the Ni-CePr catalyst had the least carbon formation associated with the greater oxygen conductivity of CePr support that facilitates carbon removal.

Apart from material selection, the influence of the microstructure of the anode on the catalytic properties under dry reforming has been investigated [89]. Two types of Ni-cermet anodes (i.e., Ni-YSZ and Ni-GDC) with different microstructure upon a sintering process at different temperature were compared. By determining the specific surface area of these anodes and through morphological observations, it was established that anode microstructure has significant impacts on the catalytic properties. The specific surface area of the anode considerably affected the CH<sub>4</sub> conversion rate whereby the cell with a Ni-YSZ anode sintered at 1200 °C which has a larger surface area gave a higher conversion rate. Another simulation study proposed an innovative SOFC configuration based on the coupling of the fuel cell and CH<sub>4</sub> dry reforming method [82]. Using Aspen Plus, the performance between the more common steam-methane-reforming (SMR)-SOFC and dry-methane-reforming (DMR)-SOFC processes was compared, where the efficiency was much better for the latter configuration with an increment of 6.4%. In another work, the prospect of co-generating electricity and CO-concentrated syngas has been demonstrated [90]. A functional layer made of a Ni<sub>0.8</sub>Co<sub>0.2</sub>-La<sub>0.2</sub>Ce<sub>0.8</sub>O<sub>1.9</sub> (NiCo-LDC) composite was added onto the anode support, and the system was fed by a CH<sub>4</sub>-CO<sub>2</sub> stream. Such a layer efficiently catalysed dry reforming in situ with CO<sub>2</sub> conversion reaching 91.5% at 700 °C and remaining stable for 100 h. Moreover, CH<sub>4</sub> was effectively converted through electrochemical oxidation, producing CO-concentrated syngas in the anode effluent. At 700 °C, maximum power density surpassed 0.91 W cm<sup>-2</sup> with a low polarisation resistance of 0.121 Ω cm<sup>2</sup>. More interestingly, this system is thermally self-sufficient, as the heat released by the H<sub>2</sub> electrochemical oxidation compensates for the requirements of the endothermic dry reforming reaction.

In addition, the performance and degradation mechanisms of a Ni-based anode-supported SOFC operating at ~800 °C on the direct internal reforming of dry CH<sub>4</sub>-CO<sub>2</sub>

mixtures have been studied by Lanzini et al. [91]. Internal reforming with CO<sub>2</sub> has been shown to be effective in reducing carbon formation with a great prospect to cogenerate syngas and concurrently treat greenhouse gases, although, similar to steam reforming, the excessive ratio between CO<sub>2</sub> and CH<sub>4</sub> would dilute the fuel, affecting the H<sub>2</sub> yield and the overall efficiency of the system [92]. Accordingly, optimal operating conditions are of great importance in order to achieve decent performance.

### 2.1.3. Partial Oxidation

Partial oxidation (POx) involves a chemical reaction between the hydrocarbon fuel and oxygen generally from the air, in a substoichiometric ratio, thus the term “partial oxidation”. This alternate approach to fuel reforming allows stable operation, where electricity and valuable chemical products such as syngas are coproduced [93,94]. However, considerable energy loss during oxidation of the hydrocarbon has caused the system with POx to be less energy efficient than with steam reforming even without heat recovery [95]. Nevertheless, the simplicity of the process makes POx attractive, i.e., for auxiliary power unit (APU) application [96].

Asano et al. applied a cell composed of Pt-BaCe<sub>0.8</sub>Y<sub>0.2</sub>O<sub>3-δ</sub>-Au operated under POx [97]. Their system did not require a separate supply of fuel and oxidant gases, as the two electrodes (Pt and Au) were exposed to the same mixture of CH<sub>4</sub> and air. Pt functions as a fuel electrode catalysing the partial oxidation of CH<sub>4</sub> to form H<sub>2</sub> and CO, whereas Au acted as an oxygen electrode. Electrochemical reduction of oxygen takes place on discharging the cell. In a uniform atmosphere, the cell produced 0.17 W cm<sup>-2</sup> at 950 °C.

An attempt to decrease the reforming temperature has been proposed by using catalytic partial oxidation (CPOx), reducing temperatures from about 1200 °C to between 800 and 900 °C, using Ni as a catalyst. Many articles related to catalysts for POx of CH<sub>4</sub> could be referred [98–100]. The state-of-the-art anode is mainly of Ni cermets, as Ni itself acts as a catalyst for the partial oxidation and at the same time functions as an electronic conductor. Nevertheless, similar to the steam and dry reforming, the use of modified Ni catalysts with elements having multiple oxidation states (e.g., Pt and Rh) for a POx process led to a better performance than using pure Ni. Employment of these catalysts led to higher reaction temperature, better fuel conversion and faster O<sub>2</sub> conversion [101]. A microtubular (MT)-SOFC consisting of an anode coated with added catalytic material coupled with a POx process demonstrated stable operation for over 1000 h [102]. Additionally, Majewski and Dhir reported steady power generation through direct feeding of CH<sub>4</sub> using a microtubular cell with a reforming catalyst placed at the cell inlet [103]. The catalyst in a honeycomb structure gave better fuel conversion with a constant rate of H<sub>2</sub> production and trivial coke deposition. They also investigated the temperature distribution along an MT-SOFC [60]. Such studies showed that not only catalyst structure could affect the SOFC performance, but the positioning of the catalyst also plays a major role in ensuring the stable operation.

A system fed with a CH<sub>4</sub>:O<sub>2</sub> ratio of 2 showed negligible carbon formation, and Ni oxidation was inhibited [104]. Cells with different anodes, Ni-YSZ or Ni-GDC, were compared, whereby in all cases, the latter had superior electrochemical performance. The maximum power densities achieved with a Ni-GDC anode were 1.35 W cm<sup>-2</sup> and 0.74 W cm<sup>-2</sup> at 650 °C and 550 °C, respectively. For Ni-GDC anode, the chemical analyses indicated that oxidation of Ni is inhibited which is due to the oxygen exchange ability of GDC. The use of various reforming agents (H<sub>2</sub>O, CO<sub>2</sub> or O<sub>2</sub>) to reform CH<sub>4</sub> was systematically studied using a cell with a Ni-ScSZ (scandia stabilised zirconia) anode and a functional layer at 850 °C [105]. It was observed that the maximum power densities of the system operated on all three gas mixtures increased initially as the ratios of CH<sub>4</sub>-to-reforming agents increased but inevitably reduced afterwards. The maximum power densities were acquired at CH<sub>4</sub>: H<sub>2</sub>O/CO<sub>2</sub>/O<sub>2</sub> ratios of 2:1, 4:1 and 8:1, respectively. Too much reforming agents result in large quantities of unconverted H<sub>2</sub>O, CO<sub>2</sub> and O<sub>2</sub> given by the poor catalytic activity of the anode. These unconverted gases diluted the fuels, reducing H<sub>2</sub>/CO concentra-



tion. Likewise, a high CH<sub>4</sub>-to-reforming-agent ratio also leads to decreased H<sub>2</sub> and CO concentrations in the fuel gas because of the low amount of these gases are formed.

Another mode of operation which combines POx and reforming either with steam or CO<sub>2</sub> could as well be applied for CH<sub>4</sub>-fuelled SOFCs. This strategy, so-called autothermal reforming (ATR), has the benefits of both processes; it is more flexible than steam reforming on start-up time and has higher efficiency than POx. By carefully controlling the ratio of steam to hydrocarbon fuel and the amount of oxygen supplied, an ATR system can achieve a self-sustaining process. The heat generated by the POx reaction provides the necessary energy for the endothermic steam reforming reaction. The resulting gas mixture, consisting of hydrogen, carbon monoxide and water vapor, is then used as a fuel for the SOFC. The effects of CO<sub>2</sub> and air addition for a system fed by CH<sub>4</sub> have also been studied through modelling [106], in which the stability, which was evaluated by monitoring the fluctuations in voltage at constant current density, was greatly influenced by carbon deposition. At 800 °C, maximum power densities of more than 1 W cm<sup>-2</sup> could be achieved with fuel streams of 75% CH<sub>4</sub>-25% CO<sub>2</sub> [106]. Mixing CH<sub>4</sub> with air as the gas inlet has also been found to increase the stability of the system. Another steady operation for 100 h has been demonstrated for a system fuelled with a 1:5 air-to-CH<sub>4</sub> ratio [107].

Some works from the literature indicate that the long-term use of Ni-based cermet anodes (i.e., Ni-YSZ and Ni-GDC) might not be appropriate for SOFCs fuelled by CH<sub>4</sub> even with internal reforming or partial oxidation. Nevertheless, suitable modification of this type of anode is always essential by incorporating suitable catalytic materials that could lower the activity for carbon formation. In addition, the optimum ratio between the reforming agent and CH<sub>4</sub> is crucial to both evade fuel dilution and suppress formation of carbon.

## 2.2. Direct Methane Utilisation

Here, we define “direct utilisation” of methane (CH<sub>4</sub>) as a process where pure or nearly pure CH<sub>4</sub> (i.e., mix with about 3% of H<sub>2</sub>O, CO<sub>2</sub> or O<sub>2</sub>) is introduced to the system, analogous to the definition adopted in a previous review [40]. This approach is possible even if the fuel does not undergo the external reforming process. A long-term steady power generation was demonstrated by a system operated with humidified CH<sub>4</sub> (3% H<sub>2</sub>O) at 1000 °C using Ni-ScSZ as anode [108]. It has also been described that during direct utilisation, gradual internal reforming (GIR) may occur by using electrochemically generated H<sub>2</sub>O and CO<sub>2</sub> [109]. This GIR concept is based on a self-sustained operation in which the water produced from the electrochemical oxidation of H<sub>2</sub> reacts in the in situ steam reforming reaction of the hydrocarbon fuel. Provided appropriate conditions are applied, direct SOFC operation with CH<sub>4</sub> using the conventional Ni-YSZ anode has also been shown to be possible [42]. Despite the encouraging performance of this Ni cermet, it is susceptible to coking, as Ni catalyses the hydrocarbon cracking. Several strategies have been proposed to inhibit carbon formation, especially when using Ni-based anodes [110]. These may be categorised into the following: stable operating conditions, modification of a Ni-based anode through surface decoration or incorporation of additional catalyst materials and application of barrier or catalytic layer, placed onto the anode. Alternatively, the use of non-Ni anodes has been actively researched as well.

### 2.2.1. Stable Operating Conditions

Several studies have reported the feasibility of operating a stable SOFC without coking through direct utilisation of CH<sub>4</sub> under controlled working conditions [42,111–113]. There are two approaches involving either operating at a high current density or applying a low working temperature, typically less than 700 °C. The latter could effectively hinder CH<sub>4</sub> cracking, whereas high current density means there are more reaction products (CO<sub>2</sub> and H<sub>2</sub>O) that could help to facilitate fuel reforming [73]. The noncoking operation can still be achieved even at higher temperatures if appropriate current density is applied [43]. Otherwise, coking is expected to occur, leading to rapid cell failure. During the SOFC operation,

the primary electrochemical reaction taking place in anodic compartment involves  $\text{CH}_4$  reforming to produce  $\text{H}_2\text{O}$  (steam) which is subsequently oxidised into  $\text{H}_2$  [43]. The resulting steam assists in removing carbon, preventing coking at high applied current densities.

The direct  $\text{CH}_4$  operation of Ni-YSZ anode-supported cell resulted in power densities of  $0.96 \text{ W cm}^{-2}$  at  $800 \text{ }^\circ\text{C}$  has been reported [42]. By assuming partial oxidation of solid carbon as part of the anodic reactions, the measured OCV value was consistent with theoretical values. A two-step reaction mechanism was proposed involving, firstly,  $\text{CH}_4$  cracking followed by the electrochemical oxidation of the resulting solid carbon. A significant buildup of carbon on the anode was suppressed by retaining an appropriate current flowing through the cell. Lin et al. studied the stability of a humidified  $\text{CH}_4$ -fuelled cell at different current densities and temperatures [43]. They observed that for operation at  $650$  and  $700 \text{ }^\circ\text{C}$ , a minimum current density of around  $0.1 \text{ A cm}^{-2}$  was necessary to retain stable operation. At higher operating temperatures, larger critical current density is needed, ranging from  $0.8$  to  $1.2 \text{ A cm}^{-2}$  and  $1.4$  to  $1.8 \text{ A cm}^{-2}$  for systems run at  $750$  and  $800 \text{ }^\circ\text{C}$ , respectively. These results showed that the oxygen ions ( $\text{O}^{2-}$ ) flux, conducted through the electrolyte, was in part accountable for hindering carbon formation and allowing steady operation.

Another research explained that a sufficient local oxygen partial pressure originated from the pumping of oxygen ions from the cathode side could as well impede the hydrocarbon cracking [114]. This “self-decoking” phenomenon has been observed in a system with a Ni-CGO anode (3:5 by weight) where the pumped oxygen ions could electrochemically remove carbonaceous deposits. A higher  $\text{CH}_4$  utilisation rate was associated with an increase in CO selectivity. Jiao et al. showed the possibility of continuous power output in a system with a Ni-YSZ anode using pure  $\text{CH}_4$ . This could be achieved by intermittent supply of  $\text{CH}_4$ , whereby fuel supply and consumption play a substantial role in controlling the carbon deposition and its utilisation [115]. This alternative operating mode is feasible in enhancing the stability of direct methane SOFCs; however, prolonged duration of such an operation must be investigated to verify its long-term stability.

### 2.2.2. Anode Surface Decoration or Incorporation of Additional Materials

Introducing another material with high ionic conductivity and excellent catalytic properties (e.g., metals or oxides) into the Ni cermet anode is another way for system optimisation. This may be realised through Ni alloying with other metals or by surface modification via various techniques including wet impregnation, electrochemical deposition (electroplating) and microwave irradiation processes. Several researchers have ascertained that alloying Ni with another element could give better carbon tolerance. This is due to the reduction in the activity of Ni when it is alloyed with another metal that has lesser catalytic activity for cracking or for activation of C-H bonds. For instance, the alloy of Ni and copper (Cu) is anticipated to improve the stability of the anode during SOFC operation with hydrocarbons by suppressing carbon formation. Copper is known to be catalytically inactive towards hydrocarbon cracking reactions but works excellently as a current collector. A cell with Ni-Cu-YSZ anodes supplied with  $\text{CH}_4$  showed the presence of carbon deposited on such alloys surface, whereby the carbon deposition was reduced with the increasing amount of Cu [39]. Similarly, a cell made of Ni-Cu-GDC [116] presented improved performance with minor carbon deposition after long-term operation with dry  $\text{CH}_4$  at  $750 \text{ }^\circ\text{C}$ . Furthermore, using Cu-Ni-samarium-doped ceria (SDC) anode-supported cell, the maximum power density of  $0.317 \text{ W cm}^{-2}$  was achieved at  $600 \text{ }^\circ\text{C}$  [117]. While losing 60% of power density after 7 h of operation in dry  $\text{CH}_4$  with bare Ni, only 7% or 2% losses were measured after 12 h when Cu was doped into the cermet or added as an interlayer, respectively. The poor performance with a pure Ni anode is mainly due to the agglomeration of Ni particles and carbon deposition.

A nanostructured Cu-Ni- $\text{CeO}_2$ -YSZ anode (i.e., Cu-Ni- $\text{CeO}_2$  impregnated into porous YSZ) has been employed which presents higher resistance to carbon deposition than the conventional Ni-based anode [118]. To assess the resilience of the Cu-Ni- $\text{CeO}_2$ -impregnated YSZ anode against coking, different types of anodes were prepared, including a blank

porous YSZ matrix, Ni-impregnated YSZ and Cu-Ni-CeO<sub>2</sub>-impregnated YSZ. The loadings of both Ni and Cu-Ni-CeO<sub>2</sub> were controlled at 40%. The results revealed a significant formation of carbon in the Ni-impregnated YSZ sample, while a reduced amount of black carbon was practical in the Cu-Ni-CeO<sub>2</sub>-impregnated YSZ sample, and no noticeable carbon deposition occurred in the porous YSZ sample. The nanostructured anode with a composition of Cu<sub>0.5</sub>Ni<sub>0.5</sub> alloy had the best performance. Hence, the content of added metal, in this case, Cu plays a significant role in suppressing problems with coking. A contradictory outcome was reported, whereby the Cu–Ni alloys were found to be unstable in the presence of hydrocarbons, depending strongly on pre-treatment conditions [119]. Thus, more research should be performed to further investigate the suitability of Cu-Ni alloy as an anode for direct CH<sub>4</sub> utilisation.

Another progress was realised using a Sn-modified Ni-based anode, whereby Sn doped with nanosized Ni and GDC were conjugated on a core GDC nanocomposite anode [120]. Operation with dry CH<sub>4</sub> produced a power density of 0.93 W cm<sup>−2</sup> and retained stable operation at 650 °C for over 40 h. Similarly, Yang et al. also used a Sn-modified Ni-based anode SOFC [121], in which a steady operation with humidified CH<sub>4</sub> is achieved in a temperature range of 700–800 °C, using a cell with an Ni-SDC anode containing additional 1 wt% Sn into the porous anode.

Introducing alkaline earth oxide materials to the Ni-cermet anode is another route to reduce carbon accumulation. Theoretically, basic oxides can increase coking resistance through stimulating the reaction of steam or CO<sub>2</sub> with the solid carbon. Asamoto et al. were among the first to study the effects of adding different alkaline earth metal oxides such as MgO, CaO, SrO and BaO to a Ni-SDC anode for direct oxidation of CH<sub>4</sub> [122]. It was found that the addition of these materials leads to lower maximum power densities compared to the bare Ni-SDC. Nevertheless, only Ni-CaO-SDC showed viable stability for 24 h operation, as indicated by minor changes in the terminal voltage.

Using BaO as part of the anode contributed to enhanced carbon tolerance caused by the discrete BaO/Ni interfaces that preferentially adsorbed H<sub>2</sub>O and gasified the carbon deposits [123]. However, there is concern about the diffusion of BaO into YSZ, leading to adverse changes in morphology and volume expansion in the YSZ grains. Hence, a novel fabrication procedure based on microwave irradiation was proposed to selectively deposit BaO solely on Ni [124]. The anode prepared via this technique shows comparable electrochemical performance using dry CH<sub>4</sub> feed to that of conventional and impregnated anodes resulting in lower carbon accumulation when operated at 800 °C. A cell comprising an anode made of Ni<sub>0.75</sub>Fe<sub>0.25</sub>–xMgO-YSZ, where x represents the weight percentage, was operated with humidified CH<sub>4</sub> as fuel at intermediate temperatures [125]. It was found that in the cell with the MgO weight percentage of 5%, a Ni<sub>0.75</sub>Fe<sub>0.25</sub>–5%MgO-YSZ anode gave the best performance, generating ~0.65 W cm<sup>−2</sup> at 800 °C.

Work by Yang et al. showed that a MgO-modified Ni-cermet anode had better tolerance towards carbon deposition [126]. A Ni-cermet anode was impregnated with a small amount of MgO (1.25 to 3.75 wt% with respect to Ni). The cell with a loading of MgO of 2.5 wt% generated a high-power density of 0.714 W cm<sup>−2</sup> and was stable for over 300 h when operated with wet CH<sub>4</sub> at 800 °C. This excellent coking tolerance was associated with the better adsorption properties of H<sub>2</sub>O and CO<sub>2</sub> on MgO as demonstrated experimentally and corroborated by density functional theory (DFT) calculations [126]. MgO is a strong Lewis base, which has a high adsorption capability for CO<sub>2</sub> to help to impede carbon deposition. This indicates that the properties of MgO could yield a paramount effect on the adsorption strength and dissociation characteristic of the involved reactants.

Liu et al. studied the doping of alkali metals (Li or Na) with NiO powder to formulate anode material with enhanced features [59]. Both Li-Ni-SDC and Na-Ni-SDC anodes have been found to increase the capability of adsorbing water vapour and CO<sub>2</sub> under cell operating conditions, enhancing coking tolerance and prevent the deactivation of the anode. The cells with modified anodes demonstrated higher OCVs, improved long-term stability and a maximum power density double that of an unmodified Ni-SDC anode.

Incorporating noble metals which are known for their excellent hydrocarbon reforming activity could as well further improve anode characteristics. A Ru-modified anode showed practical reforming activity of hydrocarbon and excellent resistance towards coking. A single cell with a Ni-GDC-3wt% Ru anode powered by dry CH<sub>4</sub> generated peak power density of 0.75 W cm<sup>-2</sup> [41]. Coking of the cell was not observed within 12 min of applied current density of 0.6 A cm<sup>-2</sup> and short exposure to the OCV condition. During fuel oxidation reactions, Pd has been described to assist in the adsorption, dissociation and diffusion processes [127,128]. The impregnated Pd transformed the inert Ni-LSC-SDC anodes to be catalytically active towards CH<sub>4</sub> oxidation [127]. In terms of predominant reaction path, the CH<sub>4</sub> activation step appears to be governed by a nonelectrochemical process on the Pd-Ni catalyst, whereas, for the noble Pd catalyst, the activation step only takes place electrochemically on active sites [127].

A cell with an anode composed of three-phase composite powders, NiO, YSZ and Ba<sub>x</sub>Zr<sub>x</sub>Y<sub>x</sub>O (BZY) prepared via spray pyrolysis was tested using dry CH<sub>4</sub> [129]. With the proper amount of BZY (which is a proton conductor), superior anode performance was observed. In addition, the impregnation of other types of proton-conducting perovskites, such as BaCe<sub>0.9</sub>Y<sub>0.1</sub>O<sub>3-δ</sub> (BCY) and BaCe<sub>0.9</sub>Yb<sub>0.1</sub>O<sub>3-δ</sub> (BCYb) into Ni-GDC has also been reported to lower polarisation and better stability of the system operated with humidified CH<sub>4</sub> by preventing carbon deposition [130].

Overall, improvement of anode properties is desirable mainly for one made from Ni cermets to make them suitable for operation with hydrocarbons. A number of reviews providing a detailed discussion on the selection, progress and the modification techniques are available in the literature for further understanding [131,132].

### 2.2.3. Anode Catalytic Layer

Barnett's group first demonstrated the idea of using a buffer layer (also termed as a catalytically active layer) applied onto the anode surface to improve system performance [133,134]. There are various terminologies which describe the additional layer, incorporated adjacent to the anode, that have been used in the literature, such as a barrier layer and anode functional layer (AFL). However, it is worth noting that in most SOFCs fuelled by H<sub>2</sub>, the AFL is aimed to reduce the activation and concentration polarisations while enlarging TPB, a region upon which the electrochemical reactions occur [135]. Furthermore, AFL for cells operated with H<sub>2</sub> often has been positioned in between the anode and the electrolyte. Meanwhile, in hydrocarbon-fuelled SOFCs, the additional layer refers to the layer that helps to transform the hydrocarbon to much simpler fuels which are often positioned on top of the anode layer. For example, on the catalyst layer, CH<sub>4</sub> is first converted into CO and H<sub>2</sub>. Next, they diffuse towards the anode on which they participate in electrochemical oxidation to produce H<sub>2</sub>O, CO<sub>2</sub> and electricity. Since CO and H<sub>2</sub> possess higher electrochemical activities than CH<sub>4</sub>, the greater cell performance is anticipated following the application of catalyst layer.

The catalyst layer is typically composed of an oxide material with a minimal tendency for coking, functioning by lowering CH<sub>4</sub> partial pressure and trapping reaction products (H<sub>2</sub>O and CO<sub>2</sub>) in the anode [133,136,137]. For instance, button cells with a barrier layer made from partially stabilised zirconia (PSZ) and ceria (CeO<sub>2</sub>) succeeded in sustaining stable and coke-free operation in a system fuelled by humidified CH<sub>4</sub> [136]. A physical model was also used to predict the performance of fuel conversion into energy in tubular cells designed with barrier layers. The model confirmed that this layer facilitates the internal reforming during operation, leading to a free-coking problem.

Murray et al. were among the first to report the direct electrochemical oxidation of CH<sub>4</sub> [36]. They tested a cell with a (Y<sub>2</sub>O<sub>3</sub>)<sub>0.15</sub>(CeO<sub>2</sub>)<sub>0.85</sub> (YDC) porous film applied onto the Ni-YSZ anode and achieved power densities of up to 0.37 W cm<sup>-2</sup> at 650 °C, and the operation was free of carbon deposition. This performance was matched with the common Ni-YSZ anode, while the YDC layer simultaneously reduced the interfacial resistance by a factor of 6. The capability of CeO<sub>2</sub> to catalyse the oxidation of hydrocarbon has been

verified [138]. No carbon deposition could occur at a temperature less than 700 °C based on the theoretical calculation for CH<sub>4</sub> pyrolysis, proposing that such reaction will not take place in that particular operating condition. Beyond 700 °C, the amount of carbon deposited increased with increasing temperatures, while less carbon deposition was detected at a given temperature on Ni-YSZ/YDC anodes than on Ni-YSZ.

A tubular cell-employing double-layer anode consisting of NiO-YSZ as a support layer and CoO-NiO-SDC as an active reforming layer was tested for the direct conversion of CH<sub>4</sub> [44]. At 800 °C, the peak power density was 0.35 W cm<sup>-2</sup>. There was no indication of carbon deposition on the surface of the anode when the cell was operated at 0.25 A cm<sup>-2</sup>. Due to its high activity, a mesoporous SDC catalyst layer impregnated with Ru showed an excellent activity for CH<sub>4</sub> electrocatalytic oxidation, achieving a maximum power density of about 0.462 W cm<sup>-2</sup> in intermediate temperature [139]. Furthermore, a catalyst layer consisting of 0.1 wt% iridium (Ir)-impregnated ceria applied onto a Ni-YSZ anode resulted in stable SOFC operation in dry CH<sub>4</sub> [47,109]. This type of a catalyst layer assisted in ensuring long-term stability for more than 200 h [109].

Depicted in Figure 5 is the principle of a gradual internal reforming (GIR) process using an anode with a catalytic layer. The process was initiated by feeding the system using 15% H<sub>2</sub> in argon. Upon reaching a steady state operation which was an hour after the start, the fuel inlet was abruptly switched to pure CH<sub>4</sub> [140]. The same author also applied a model with the CFD-Ace software (<https://www.esi.com.au/software/cfd-ace/>) to further investigate the GIR process at the anode. From a thermodynamic perspective, a system with a catalyst layer as reported in their earlier work effectively allows GIR without coking when fuelled with either pure CH<sub>4</sub> or using a mixture with a small quantity of steam [140].

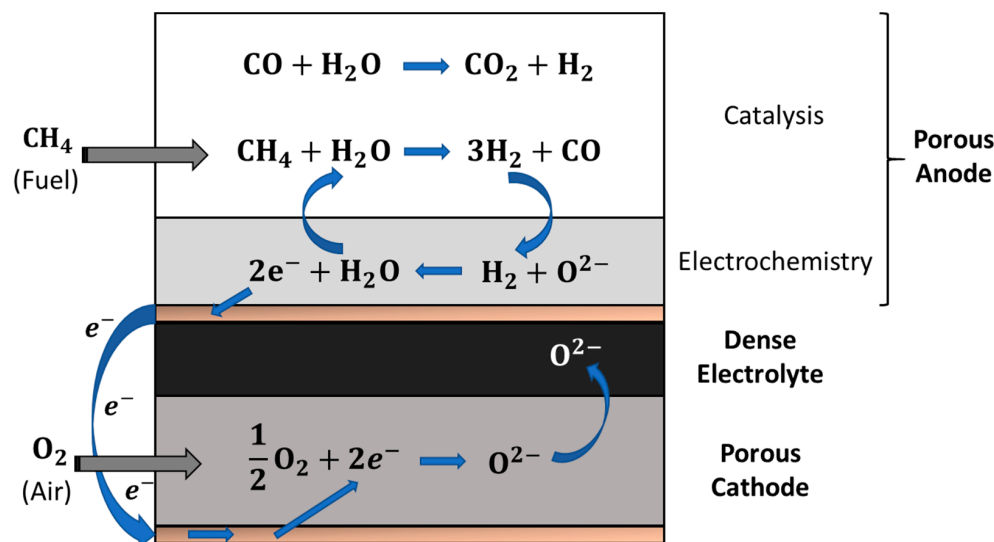


Figure 5. Principal of gradual internal reforming (GIR) process by anode with a catalyst layer.

The performance of a single cell with a  $\gamma$ -Al<sub>2</sub>O<sub>3</sub> layer placed onto a Ni-based anode presented a peak power density of 0.382 W cm<sup>-2</sup> at 850 °C, more than double that of its counterpart without such a layer. This layer also assisted in sustaining stable operation with no carbon formation [141]. A strategy of having catalytic materials used as part of the anode and as a functional layer has been demonstrated [142], where Sn-doped Ni-YSZ was used as both an anode catalyst and a functional layer. This functional layer was sandwiched between the anode and electrolyte, creating a system capable of operating in an intermediate temperature range with a reasonably good power density. The cell achieved 0.41 W cm<sup>-2</sup> when operated with humidified CH<sub>4</sub> at 650 °C. A comparison with a cell without Sn indicated that the stability of the operation is much better, as the Sn-doped Ni-YSZ cell worked for 137 h, while the Ni-YSZ cell ceased operation within 27 h. Alloying Ni with Fe is expected to assist in resisting carbon deposition due to lower activities of



Fe. It was observed for a cell with a Ni-Fe alloy catalyst layer on top of the Ni-YSZ anode, operated with 97% CH<sub>4</sub>-3% H<sub>2</sub>O as fuel, the additional Ni-Fe layer was effective for CH<sub>4</sub> internal reforming in SOFC systems [143].

Direct internal reforming (DIR), as shown in Figure 2d, involves adding a reforming function to the anode and the reforming agent(s) (e.g., steam or CO<sub>2</sub>) is supplied together with the hydrocarbon fuel. In this case, an important aspect of the steam-to-carbon ratio must be superior to 1 to prevent coking. As countermeasure to the thermal stress induced within the cell under DIR configuration as described in Section 1.1, new mode of operation has been initiated. Gradual internal reforming (GIR), such as DIR, is based on the synergy between fuel steam reforming taking place on a catalytic layer anode (Ni) and electrochemical oxidation of hydrogen occurring at the electrode's triple-phase. In both the GIR and DIR modes, hydrogen which is required by the electrochemical reaction is continuously generated in situ. They both also suffer from CO<sub>2</sub> production via water-gas shift reaction as depicted in Figure 5. However, unlike DIR which necessitates substantial amount of steam, the GIR process requires small quantity of steam at its fuel inlet, to the point where the steam electrochemically generated within the cell is adequate for the reforming reaction. This approach was the foundation of the works reported by Vernoux et al. [144] and Georges et al. [145] through which they had studied the feasibility of GIR in SOFCs. It has also been reported that an SOFC fuelled by CH<sub>4</sub> for a continuous period of 400 h without adding water, O<sub>2</sub> or CO<sub>2</sub> successfully delivered relatively stable power output [146].

### 3. Heavier Hydrocarbon-Fuelled SOFCs

Compared to CH<sub>4</sub>, the use of heavier hydrocarbons as a fuel for SOFCs appears to be more challenging, as it involves even more complex reactions. It has been recognised that carbon formation could damage the Ni-based anodes [147,148]. Particularly at high SOFC operating temperatures, carbon deposition is more likely to occur when using heavier hydrocarbons than CH<sub>4</sub> [149]. Even so, these fuels remain desirable from the perspective of fuel economy [150]; thus, various strategies have been attempted.

There are three ways to utilise heavier hydrocarbons as fuel for SOFCs. First, they may be partially and externally reformed, producing a highly concentrated CH<sub>4</sub> mixture which is then fed and internally reformed [96,151]. This is analogous to CH<sub>4</sub> internal reforming as deliberated in the previous section and is not discussed further below. Second, hydrocarbons can undergo an internal reforming process in which they are first mixed with reforming agents (either H<sub>2</sub>O, CO<sub>2</sub> or air) before being supplied to the system. Third, a pure or nearly pure hydrocarbon (humidified with ~3% vol. H<sub>2</sub>O) may be introduced directly into the anode compartment. This mode of operation greatly depends on the properties and the ability of the anode material to suppress the formation of carbon. The following sections discuss the different approaches to the use of heavier hydrocarbons in SOFCs.

#### 3.1. Internal Reforming

Internal reforming of heavier hydrocarbons for SOFCs is attractive for a simplified power generation system. A similar approach to a CH<sub>4</sub>-fuelled system could also be applied for the operation with heavier hydrocarbons, in which the fuel could be mixed with different reforming agent, i.e., steam, CO<sub>2</sub> or O<sub>2</sub>, before entering the anode compartment.

##### 3.1.1. Internal Steam and Dry Reforming

The practicality of internal reforming of heavier hydrocarbons has been reported [149–152], contrary to the earlier report that claimed that only CH<sub>4</sub> could be internally reformed [153]. A study on the direct use of n-dodecane (C<sub>12</sub>H<sub>26</sub>) has been conducted using cells with a Ni-ScSZ-cermet anode [149]. At a steam-to-carbon (S/C) ratio between 1 and 2, a steady operation at 0.1 A and nearly 45% fuel utilisation are attained with anode potential of approximately 0.77 V. No degradation of both the anode and current collector was observed. Similarly, stable operation is perceived at a lower S/C ratio of 0.5, but the Ni mesh current collector was partially disintegrated due to the metal dusting. The thermal

decomposition of  $n\text{-C}_{12}\text{H}_{26}$  formed  $\text{C}_2\text{H}_4$  and  $\text{H}_2$  as major products with negligible coke deposition. This was followed by steam reforming of hydrocarbons, CO shift reaction and  $\text{H}_2$  electrochemical oxidation. The first two reactions turned out to be hostile at a low S/C ratio. Nevertheless, these reactions could be promoted with increasing fuel utilisation, and carbon deposition at the outlet tube is restrained although reforming reactions of hydrocarbons were incomplete.

The influence of steam and discharge conditions onto internal reforming of propane ( $\text{C}_3\text{H}_8$ ) was studied using different types of Ni-based anodes [150]. Even at a high S/C ratio, power generation characteristics with a Ni-YSZ anode were declined at  $1000\text{ }^\circ\text{C}$  due to carbon formation at low current densities. By contrast, stable operation at an S/C ratio of 0.8 was obtained when using either Ni-ScSZ or Ni-samaria-doped ceria (SDC) anode. At low S/C ratio operation, the carbon deposition rate was lower for a cell with a Ni-ScSZ anode than with Ni-YSZ. The overall performance analysis showed that the stability of Ni-based cermet was in the order of Ni-ScSZ > Ni-YSZ > Ni-SDC.

The addition of noble metals is envisioned to promote catalytic properties further during steam reforming [154]. This was demonstrated by the slower deterioration of anodes incorporated with Ru (i.e., Ru-Ni-YSZ and Ru-YSZ anodes) than the unmodified Ni-YSZ anode [150]. In another study, the degree of internal steam reforming activities for Ni-GDC and Ni-YSZ with butane ( $\text{C}_4\text{H}_{10}$ ) at  $600\text{ }^\circ\text{C}$  was compared, and the former was found to have better output [152]. However, the  $\text{C}_4\text{H}_{10}$  conversion was incomplete, as the gas hourly space velocity was low. To encourage fuel conversion, various dopants such as Cu, Sn and Rh were added to the NiO-GDC anode. Among these, the Rh-modified anode presented a complete conversion of  $\text{C}_4\text{H}_{10}$  without coking during operation with a S/C ratio set at 3 and showed a very low degradation rate when operated in an internal reforming mode.

A survey of the literature described that the presence of a catalyst layer combined with the internal reforming led to a better system performance. For example, two different structures of ceria (mesoporous powders and mesoporous flower-like microspheres), each was used to form a reforming catalyst layer and tested with a fuel mixture of 5% iso-octane, 9% air, 3%  $\text{H}_2\text{O}$  and 83%  $\text{CO}_2$ . In comparison, the cell with a flower-like mesoporous  $\text{CeO}_2\text{-Ru}$  microsphere catalyst layer demonstrated superior performance, yielding a maximum power density up to  $0.654\text{ W cm}^{-2}$  at  $600\text{ }^\circ\text{C}$  [155]. It is, however, worth noting that the high fraction of  $\text{CO}_2$  added (as part of the agent for reforming processes) could also be responsible for the improved power output.

The direct utilisation of iso-octane ( $\text{C}_8\text{H}_{18}$ ) in an SOFC with a multifunctional anode (made of two layers) without cofeeding  $\text{O}_2$  or  $\text{CO}_2$  has also been described [156]. Unlike previous works which require a considerable amount of  $\text{O}_2$  (typically from the air) or  $\text{CO}_2$  to minimise coking and anode deactivation [134,155,157,158], a fuel mixture with a  $\text{H}_2\text{O-to-C}_8\text{H}_{18}$  ratio of  $\sim 0.5$  was applied. This ratio is much lower than the ideal value of 8 for steam reforming. These dual-layer anodes have their specific functions, wherein the outer catalyst layer is used to reform the hydrocarbon fuels, while the inner active layer (adjacent to the electrolyte) provides sites for the electrochemical oxidation of the reformed fuels.

### 3.1.2. Partial Oxidation

SOFCs with an incorporated catalyst layer placed on top of the anode that allows partial oxidation have shown to be advantageous. Partial oxidation (POx) of  $\text{C}_3\text{H}_8$  on a Ni-YSZ anode [159] and a Ru-based catalyst layer applied on the anode [160] have been demonstrated. Zhan and Barnett were those who initiated the idea and implemented this approach by utilising a porous PSZ anode supported cell operated by  $\text{C}_3\text{H}_8$  [160]. A Ru- $\text{CeO}_2$  catalyst layer applied onto the PSZ surface catalysed the partial oxidation of  $\text{C}_3\text{H}_8$  at temperatures higher than  $500\text{ }^\circ\text{C}$ . The same authors also reported the practicality of using iso- $\text{C}_8\text{H}_{18}$ , a high-purity compound similar to gasoline, for SOFCs [134,158,161]. The use of a porous PSZ or PSZ/ $\text{CeO}_2$  disc positioned in between two Ru/ $\text{CeO}_2$  layers was effective in hindering coking attributable to active  $\text{CO}_2$ -reforming of iso- $\text{C}_8\text{H}_{18}$  [134]. A

similar catalyst layer applied on top of a thick Ni-SDC anode contributed to a stable power density of  $0.6 \text{ W cm}^{-2}$  at  $590 \text{ }^\circ\text{C}$  with no sign of carbon formation.

In addition, this synergic method is reported to be effective for in situ reforming of various fuels including natural gas, propane ( $\text{C}_3\text{H}_8$ ), butane ( $\text{C}_4\text{H}_{10}$ ) and biomass in a tubular cell system [102]. An SOFC with four-layer internal reforming was found to be efficient in generating high power densities with stable operation. However, for proprietary reasons, the exact composition for the catalytic layer could not be disclosed by the authors.

Overall, the works discussed above show that the integrated catalyst layer is effective in stimulating the reforming process which allows a noncoking operation with steady power output. Although most of the studies reported in the literature were conducted in a small-scale, the obtained information was useful in providing better insight into internal reforming of heavier hydrocarbons during SOFC operation.

### 3.2. Direct Hydrocarbon Utilisation

Extensive efforts have been directed towards the direct use of hydrocarbons for the simplicity of the SOFC system. As larger hydrocarbons impose a greater challenge in direct use, a noncoking anode composition along with a synergistic approach to minimising coking is thus anticipated. Earlier, Park and coworkers demonstrated that operation with dry hydrocarbons including liquid fuels is possible, even without undergoing a reforming process [26]. Different types of hydrocarbons such as  $\text{CH}_4$ ,  $\text{C}_2\text{H}_6$ , 1-butene ( $\text{C}_4\text{H}_8$ ),  $n\text{-C}_4\text{H}_{10}$  and toluene ( $\text{C}_7\text{H}_8$ ) were tested using cells with a composite anode of Cu and  $\text{CeO}_2$  (or Sm-doped  $\text{CeO}_2$ ) operated at  $700$  and  $800 \text{ }^\circ\text{C}$ . Stable operation with no indication of coking on the anode surface is perceived and the final products of the oxidation were  $\text{CO}_2$  and water. However, the measured power density of a system fuelled by  $n\text{-C}_4\text{H}_{10}$  was relatively lower than that operated with  $\text{H}_2$ .

It has been proposed that the direct oxidation of various hydrocarbons (i.e.,  $\text{CH}_4$ ,  $\text{C}_2\text{H}_6$  and  $\text{C}_3\text{H}_8$ ) was interrupted by the steam and  $\text{CO}_2$  formed as products of the electrochemical reaction [37,41]. Hence, these two components should be removed from the anode surface. This can be achieved by internally reforming unreacted hydrocarbons to further promote the electrochemical oxidation. To verify this assertion, the performance of a Ni-GDC anode modified by different catalysts such as Pt, Pd, Cu, Rh and Ru was studied by directly supply hydrocarbons to the system at  $600 \text{ }^\circ\text{C}$ . These metal-modified anodes facilitate the reforming of the unreacted hydrocarbons using the generated steam and  $\text{CO}_2$ , leading to better system efficiency. Interestingly, a system operated with dry  $\text{CH}_4$  showed a comparable performance to one using humidified  $\text{H}_2$ .

The direct use of  $5.3 \text{ vol.}\%$   $\text{C}_8\text{H}_{18}$  in  $\text{N}_2$  was studied over a temperature range of  $600$  and  $775 \text{ }^\circ\text{C}$  [162]. Mass spectroscopy analysis indicated the presence of  $\text{CH}_4$  and  $\text{C}_2\text{H}_2$ ; both were the main products of  $\text{C}_8\text{H}_{18}$  thermal decomposition in the electrochemical reactions. An SOFC with Ni-YSZ anode was proposed to be operated below  $750 \text{ }^\circ\text{C}$  for stable operation without coking. In another study, the influence of  $\text{C}_2\text{H}_6$  and  $\text{C}_3\text{H}_8$  in a simulated natural gas on the operation of a Ni-YSZ anode-supported SOFC was examined [66]. Incorporating a diffusion barrier layer made of PSZ, which has excellent catalytic properties, should stimulate the reforming reaction of hydrocarbons. This is verified as it was detected that  $\text{H}_2$ -rich gases reach the anode surface instead of hydrocarbon fuels. A system fed by natural gas with  $5\%$   $\text{C}_2\text{H}_6$  and  $2.5\%$   $\text{C}_3\text{H}_8$  and the additional  $33\%$  of air at  $750 \text{ }^\circ\text{C}$  demonstrated stable operation, and no noticeable coking was detected.

Another strategy to control carbon formation is by creating nanostructured BaO/Ni interfaces on the anode through a vapour deposition method, where the promotion of water-mediated carbon removal in a system fuelled with dry  $\text{C}_3\text{H}_8$  at  $750 \text{ }^\circ\text{C}$  was demonstrated [163]. The system produced a constant peak power density of  $0.88 \text{ W cm}^{-2}$ . A main benefit of this BaO vapour deposition is that it can be readily integrated into existing processes for preparing SOFCs, as it does not require extra processing steps.

It has also been reported that composite oxide anodes, doped  $\text{CeO}_2\text{-LaFeO}_3$  ( $\text{Ce}(\text{Mn}, \text{Fe})\text{O}_2\text{-La}(\text{Sr})\text{Fe}(\text{Mn})\text{O}_3$ ), displayed promising results in a system fed by either dry  $\text{C}_3\text{H}_8$  or

dry  $C_4H_{10}$  [27]. After a long-term test, the system generated consistent power densities of approximately  $1\text{ W cm}^{-2}$  at  $800\text{ }^\circ\text{C}$  with no observable carbon deposit. In another work, the same authors achieved even better performance using a similar composite anode, but with the addition of  $RuO_2$  as a catalyst [164]. An anode consisting of 10 wt%  $RuO_2$  contributed to a power density of  $1.5\text{ W cm}^{-2}$  when fuelled with dry  $C_3H_8$  at  $800\text{ }^\circ\text{C}$  and operated stably for 50 h without noticeable carbon deposition.

In contradiction of the renowned deleterious impact of coking on cell performance, the formation of carbonaceous residues within the Cu-CeO<sub>2</sub>-YSZ anode upon exposure to n-C<sub>4</sub>H<sub>10</sub> at  $700\text{ }^\circ\text{C}$  was found to offer better energy output [147]. During operation with n-C<sub>4</sub>H<sub>10</sub>, polyaromatic compounds (tars) formed from the vapour phase and free radical reactions are deposited on the anode surface. Although the formation rate is insignificant at and below  $700\text{ }^\circ\text{C}$ , it becomes more apparent beyond this temperature. At  $700\text{ }^\circ\text{C}$ , the sufficient amounts of tar formed over a short period help to improve performance by allowing supplementary electronic conductivity [147,148,165]. However, with extended operation, the increased amount of tar deposit became more stable and damaging to the anode functionality. In addition, tar deposition will gradually block the active sites compromising the electrochemical performance. Thus, avoiding carbon formation is necessary to ensure long-term stability of the SOFC system fuelled by the heavy hydrocarbons.

Analysis of the carbon removal could be performed using a mass spectrometer by referring to the amount of CO<sub>2</sub> produced (represented by  $m/e = 44$ ) [147]. As shown in Figure 6, exposure to oxidising gas (20% O<sub>2</sub> in a He carrier) at a range of operating temperatures could eliminate the deposits. The amount of CO<sub>2</sub> increases with the applied temperature. In contrast, it was reported that the removal of these deposits using steam requires much higher temperatures ( $>900\text{ }^\circ\text{C}$ ) [147]. These findings show that such an SOFC would have to be regenerated periodically by a redox cycle, particularly when fuelled with hydrocarbons for long-term use. These cells, unfortunately, have yet to be able to generate power densities comparable to those with Ni-based anodes. This is partly because the operating temperature must be kept at  $700\text{ }^\circ\text{C}$  to curtail carbon deposition. Lower temperatures may affect the reactions kinetic and the conductivity of the electrolyte depending on the material used for making the cell.

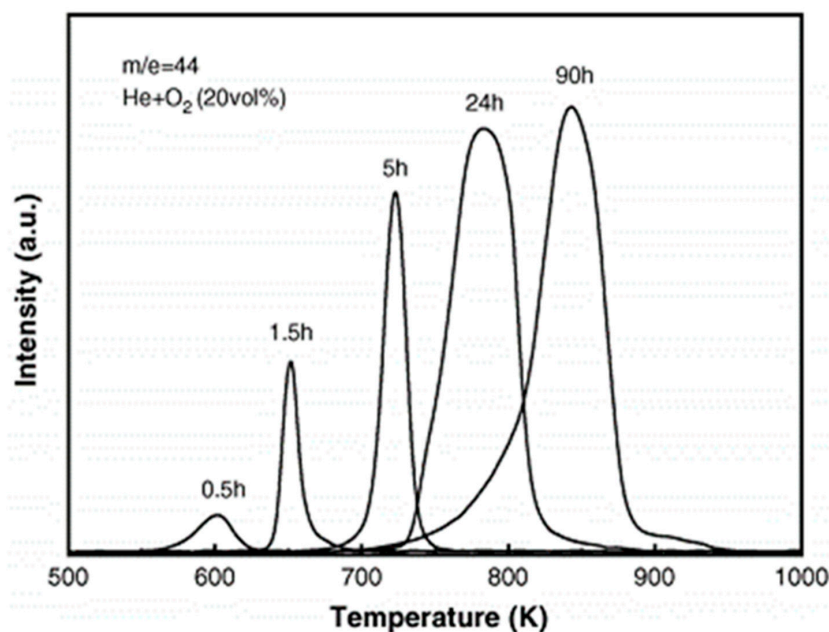


**Figure 6.** Temperature-programme oxidation (TPO) curves in oxidising gas with porous YSZ-CeO<sub>2</sub> exposed to n-butane at  $973\text{ K}$  for different periods. Figure is adapted from [147].

The use of heavier hydrocarbons is intriguing as they originate from a variety of sources with reasonable prices. Those in liquid form may help to resolve transportation difficulties. However, the chemistry behind the electrochemical reactions of these hydrocarbons during SOFC operation is still not fully understood. Ongoing research on the reaction mechanism, control, impurities issues as well as the requirement for a robust catalyst with adequate lifespan is necessary if this technology is to be applied commercially. Table 3 lists the electrochemical performance parameters of heavier hydrocarbon-fuelled SOFCs, showing some cells with decent power densities reported.

**Table 3.** Heavier hydrocarbons-fuelled SOFCs.

Anode	Electrolyte	Cathode	Fuel Stream	Temp. (°C)	OCV (V)	Max. Power Density (W·cm <sup>-2</sup> )	Ref.
Cu-CeO <sub>2</sub> -YSZ	YSZ (~20 μm)	LSM	C <sub>4</sub> H <sub>10</sub>	700	1.0	0.14	[40] [166]
Cu-CeO <sub>2</sub> -YSZ	YSZ (60 μm)	LSM-YSZ	Dry n-C <sub>4</sub> H <sub>10</sub>	800 700	~0.9	0.18 0.12	[26]
Ru-Ni-GDC	GDC (~40 μm)	SSC	Dry C <sub>2</sub> H <sub>6</sub> Dry C <sub>3</sub> H <sub>8</sub>	600	0.85–0.9	0.716 0.648	[37]
Ni-GDC-Ru	GDC	SSC	Dry C <sub>2</sub> H <sub>6</sub> Dry C <sub>3</sub> H <sub>8</sub>	600	0.9	0.716 0.648	[41]
Cu-CeO <sub>2</sub> -SDC	SDC (380 μm)	SDC-LSCF	Dry C <sub>4</sub> H <sub>10</sub>	700	0.794	0.170	[167]
Ni-SDC (700 μm)	SDC (20 μm)	BSCF-SDC	C <sub>3</sub> H <sub>8</sub> :O <sub>2</sub> :He 4:9:36 vol. ratio (ml min <sup>-1</sup> )	500	~0.68	~0.44	[168]
Cu-CeO <sub>2</sub> -SDC Cu-CeO <sub>2</sub> -LSGM Cu-CeO <sub>2</sub> -ScSZ	SDC LSGM ScSZ	SDC-LSCF LSGM-LSCF LSM-ScSZ	Dry n-C <sub>4</sub> H <sub>10</sub>	700	−1.0	0.18 ~0.09 0.15	[169]
Cu <sub>0.5</sub> Co <sub>0.5</sub> -CeO <sub>2</sub> -YSZ	YSZ (60 μm)	YSZ-LSM	Dry C <sub>4</sub> H <sub>10</sub>	700 800	1.1	~0.14 0.36	[119]
Cu-CeO <sub>2</sub> -LSGM	LSGM (440 μm)	LSCF-LSGM (50:50 wt%)	Dry C <sub>4</sub> H <sub>10</sub>	700	1.06	0.115	[170]
NiO-YSZ	YSZ	LSCF-GDC/LSCF	iso-C <sub>8</sub> H <sub>18</sub> :air: CO <sub>2</sub> (5:9:86)	570 670 770	0.97 to 1.02	0.1 0.3 0.6	[134]
NiO-SDC	SDC			570	~0.82	~0.35	
NiO-YSZ-PSZ	YSZ	LSCF-GDC	C <sub>3</sub> H <sub>8</sub> : O <sub>2</sub> : Ar (10.7:18.7:70.6)	750	~0.92	~0.48	[160]
NiO-SDC	SDC	LSCF-SDC	iso-C <sub>8</sub> H <sub>18</sub> : air (6:94)	590 640	~0.8	0.6 0.68	[158]
Cu-CeO <sub>2</sub> -YSZ	YSZ (60 μm)	LSM-YSZ	n-C <sub>10</sub> H <sub>22</sub>	700 750 800	1.0	0.1 0.17 0.24	[148]
BaO/Ni-YSZ	YSZ (~15 μm)	SDC-LSCF	Dry C <sub>3</sub> H <sub>8</sub>	750	~1.0	0.88	[163]
Ni-GDC	YSZ/GDC interlayer	LSCF	C <sub>4</sub> H <sub>10</sub> /H <sub>2</sub> O (S/C = 0.044)	610	1.05	0.26	[55]
Ni-YSZ-BZY-Ni-YSZ	YSZ-SDC	LSCF	Wet iso-C <sub>8</sub> H <sub>18</sub> (6.5%inAr) (S/C ratio of 1/17)	750	~1.05	0.6	[156]
Cu-Fe/ceria-YSZ	YSZ	YSZ-LSM	n-C <sub>4</sub> H <sub>10</sub>	800	~1.18	0.240	[171]
CMF-LSFM CMF-LSFM + 10 wt% RuO <sub>2</sub>	LSGMC (~0.3 mm)	SSC	C <sub>3</sub> H <sub>8</sub>	800	1.09 1.122	1.08 1.583	[164]
Ni-GDC Rh-Ni-GDC	GDC (1.3 ± 0.1 mm)	PSCF3737	n-C <sub>4</sub> H <sub>10</sub> :steam:N <sub>2</sub> (10:120:70)	600	0.9–0.95	~0.011 ~0.024	[152]
Ni-SDC	ScCeSZ (12 μm)	Pr <sub>6</sub> O <sub>11</sub> -P434L alloy	45% C <sub>2</sub> H <sub>5</sub> OH–55% H <sub>2</sub> O	700	~1.01	0.87	[172]

Ba<sub>0.5</sub>Sr<sub>0.5</sub>-Co<sub>0.8</sub>Fe<sub>0.2</sub>O<sub>3-δ</sub> (BSCF); BaZr<sub>1-x</sub>Y<sub>x</sub>O<sub>3-δ</sub> (BZY); Ce<sub>0.6</sub>Mn<sub>0.3</sub>Fe<sub>0.1</sub>O<sub>2</sub>-La<sub>0.6</sub>Sr<sub>0.4</sub>Fe<sub>0.9</sub>Mn<sub>0.1</sub>O<sub>3</sub> (CMF-LSFM); La<sub>0.8</sub>Sr<sub>0.2</sub>Ga<sub>0.8</sub>Mg<sub>0.15</sub>Co<sub>0.05</sub>O<sub>3</sub> (LSGMC); Pr<sub>0.3</sub>Sr<sub>0.7</sub>Co<sub>0.3</sub>Fe<sub>0.7</sub>O<sub>3</sub> (PSCF3737); Sm<sub>0.5</sub>Sr<sub>0.5</sub>CoO<sub>3</sub> (SSC); scandia-ceria-stabilized zirconia (ScCeSZ).



#### 4. Current and Future Trends of Research on Hydrocarbon-Fuelled SOFCs

A fuel cell is an environmentally friendly alternative to the conventional combustion technology for energy generation. Especially with SOFCs, high working temperatures allow such systems to use a wide variety of fuel intake including hydrocarbons. The possibility of utilising hydrocarbons presents a substantial benefit against other low-temperature fuel cell counterparts. For decades, SOFCs technology has been continuously, if not rapidly, progressing. Numerous aspects are constantly being explored and improved [173]. While many improvements have been achieved, the issues of cost, durability, stability and sustainable electrochemical performance remain as major challenges. Until now, Ni-based anodes for hydrocarbon-fuelled SOFCs have garnered the most extensive global research attention. Nevertheless, recent attempt to implement the  $\text{LiNi}_{0.8}\text{Co}_{0.15}\text{Al}_{0.05}\text{O}_2$  anode under  $\text{CH}_4$ -fuelled conditions have demonstrated instability, manifesting through its decomposition [174]. While endeavours to enhance and modify Ni-based anodes persist, the pursuit of alternatives of Ni-based cermets as anode materials for a hydrocarbon-fuelled system is required to resolve coking issues and ensure long-term stability [175]. Direct utilisation of hydrocarbons has become a key feature that may allow SOFCs to be commercialised as current impediments include the high cost of  $\text{H}_2$  production along with its safety and environmental concerns. In addition, with regards to sustainable development, the fuel flexibility of this technology also presents a promising transition from fossil to renewable fuels.

##### 4.1. Use of Non-Ni Anode Materials

As a fuel electrode, an anode must not only be able to catalyse the electrochemical oxidation of the hydrocarbon fuel but also have the ability to withstand SOFC operating conditions. In recent years, there has been a proposition to apply nickel-free anodes such as other types of cermet (i.e., Cu-CeO<sub>2</sub>) [176] or perovskite-based for operation with hydrocarbons [177]. Numerous lab-scale studies with these anodes have described consistent cell performance with possible noncoking operation. For instance, Cu-CeO<sub>2</sub> and perovskites such as  $\text{La}_{0.75}\text{Sr}_{0.25}\text{Cr}_{0.5}\text{Mn}_{0.5}\text{O}_{3-\delta}$  (LSCM) [177] have been reported to present stable SOFC operation with wet methane. For the former, researchers from the University of Pennsylvania have developed SOFCs with copper (Cu)-based anodes with ceria (CeO<sub>2</sub>) as catalyst and tested them with various hydrocarbons, where good cell performance and noncoking condition have been demonstrated [20,40,166,178]. Their cell was developed by forming the porous YSZ matrix using dual-tape-casting technique then followed by the impregnation of Cu and CeO<sub>2</sub> using nitrate-based solutions. Following that was the decomposition and reduction processes to form Cu-CeO<sub>2</sub>-YSZ composites [20]. Copper and ceria have their own functionalities as a current collector and catalyst for the fuel electrochemical reactions, respectively. Copper is a poor catalyst for breaking C-H bonds, and its ability to form C-C bonds is restricted, and these may be the causes of noncoking operation. The OCV acquired, however, remains much lower than that estimated by thermodynamics. This alludes that the conversion of hydrocarbon involves a route other than direct oxidation, viz., through hydrocarbon cracking and subsequently the electrochemical oxidation of cracked products.

During operation at 700 °C with Cu-CeO<sub>2</sub>-YSZ cermet anodes for the oxidation of various types of hydrocarbons such as methane, propane, butane, decane and toluene, cells containing less than 20 wt% Cu in the cermet anode structure demonstrated improved cell performance that further enhanced over time. This was attributed to enhanced electrical connectivity owing to the formation of carbonaceous deposits within the pores of the cermet anode that link the Cu particles together for better percolation [148,165]. This observation is in agreement with other works on enhanced cell performance caused by the carbon deposits during  $\text{CH}_4$  oxidation on Cu-based anodes.

Alternatively, the use of oxide materials as anode materials allows the prospect that all cell components to be derived from ceramic materials, making the fabrication and processing of the cell simple and easier. More interesting, they do not form carbon under

most conditions and could solve issues of redox stability. These oxide materials can be categorised according to their crystalline structures: fluorite (e.g., zirconia- and ceria-based), rutile, tungsten bronze, pyrochlore, perovskites (e.g., chromite, titanate and vanadate) and double perovskites [179]. Remarkable progress has been reported in recent years, as most perovskite and perovskite-related structures that are often applied as a cathode are now being tested for making anode. With this development, the anode may be made of a single component contrasted with cermets, resolving disputes such as thermal expansion mismatches and solid-state reactions between the cell components. Ge et al. [110] indicated that SOFC's oxide anode materials could be assessed qualitatively using a "performance tetrahedron" whose four vertices are electrical conductivity, electrocatalytic activity, redox stability and fuel flexibility.

Among various oxide types, the most common are those of perovskite and double perovskite structures. Several potential candidates include  $\text{La}_{0.8}\text{Sr}_{0.2}\text{Cr}_{0.5}\text{Mn}_{0.5}\text{O}_3$  (LSCM), Mn and Ga codoped LST (lanthanum strontium titanate),  $\text{La}_4\text{Sr}_8\text{Ti}_{11}\text{Mn}_{0.5}\text{Ga}_{0.5}\text{O}_{37.5}$  (LSTMG),  $\text{La}_{1-x}\text{Sr}_x\text{VO}_3$  (LSV),  $\text{Sr}_2\text{Mg}_{1-x}\text{Mo}_x\text{O}_{6-\delta}$  (SMMO) and  $\text{Sr}_2\text{MoFeO}_{6-\delta}$  (SMFO) [110]. As detailed discussion on these possible anode materials are beyond the scope of this review, interested readers are directed to several excellent reviews for more information [12,18,110,179–181]. Indeed, issues concerning the electrical conductivity of LSCM, LSTMG and SMMO, the thermal stability of SMMO and SMFO and redox stability of LSV and SMMO remain as great challenges, but further improvement of such issues is continuing. Oxide materials have shown encouraging power output and exceptional redox stability at high temperatures, typically beyond 700 °C. Catalytic activity, however, declines promptly with temperature, and these materials cannot at the moment work well in the intermediate temperature range. Despite this encouraging progress, these materials are, at this point, more costly than the regularly applied Ni cermets. In addition, the use of these oxides as anodes yielded relatively lower power density (between 0.2 and 0.44 W cm<sup>-2</sup>) at 800–900 °C compared to the Ni-based anode.

It is noteworthy that there is a trade-off between deficiency in carbon deposition and sufficient electrochemical activity. Anodes that do not catalyse carbon formation incline to be less reactive for the electrochemical oxidation or vice versa. Nevertheless, the use of redox stable metal oxides as anodes appears to be exciting. This field of research may see major advances in the future, but until these materials have been properly developed and their characteristics in harsh SOFC operating atmospheres are well-understood, cermets will remain the material of choice for making anode.

#### 4.2. Strategies for Stable SOFC Operation

Apprehension about the system's durability and stability should also be taken into thoughtful consideration. For a success in the marketplace, SOFCs must be economical and present a decent lifespan. Long-term stability is necessary to be competitive means for energy generation against the conventional combustion technology. Essentially, materials applied for an SOFC should be robust and able to function properly for continuous operation in harsh conditions. Latest emergence of perovskite-based material has been intriguing, but before being considered practical, issues surrounding the cost and fabrication process must be resolved to allow large-scale production with economic benefits [9].

It has been commonly accepted that the activity of SOFC anodes is dependent not only on materials of electrode but also on its morphology as well as operating environments [182]. It has been recognised that the reliability, durability and stability of the SOFCs could be markedly improved by decreasing their working temperature. There are concerns with regards to high-temperature operation ( $\geq 750$  °C) including the strictly limited selection of material, electrode sintering and the interfacial diffusion between cell components. Hence, it is of great interest to operate the system in an intermediate range of temperatures, i.e., 550 to 750 °C [183,184]. Lowering the working temperature could certainly allow more choice of SOFC materials. Studies have demonstrated that the operation at lower temperatures (<800 °C) for cells with Ni-based anodes are likely with thin YSZ electrolytes [185] or using

highly conducting electrolytes such as GDC and doped LaGaO<sub>3</sub> [186]. In addition, applying SOFCs at a low-temperature range ( $\leq 650$  °C) has received lots of attention to directly use hydrocarbons as fuels. For instance, performance degradation caused by carbon formation during the direct use of CH<sub>4</sub> could be avoided through the addition of an internal reforming layer composed of Ni supported on proton-conducting La-doped ceria (i.e., La<sub>2</sub>Ce<sub>2</sub>O<sub>7</sub> (LDC) and La<sub>1.95</sub>Sm<sub>0.05</sub>Ce<sub>2</sub>O<sub>7</sub> (LSDC)) which was applied over Ni-Ce<sub>0.8</sub>Sm<sub>0.2</sub>O<sub>2-x</sub> (SDC) anodes. Such a proton-conducting layer can adsorb water for internal reforming and therefore considerably improve the performance of the direct methane SOFCs.

Another emerging proton-conducting material for making an SOFC is BaZr<sub>0.1</sub>Ce<sub>0.7</sub>Y<sub>0.1</sub>Yb<sub>0.1</sub>O<sub>3- $\delta$</sub>  (BZCYYb). Using a NiO-BZCYYb anode with an additional LaNi<sub>0.6</sub>Co<sub>0.4</sub>O<sub>3</sub> anode functional layer and a thin BZCYYb electrolyte, stable operation for 200 h has been demonstrated when operated under wet CH<sub>4</sub> at 550 °C [61]. Review by Su and Hu summarises the most recent advances in hydrocarbon-fuelled SOFCs operating at 650 °C, with a particular emphasis on the challenges and strategies associated with the cells components [8]. It has been highlighted on the requirement for highly active and carbon/sulphur resistant anodes, as well as highly ionic conductive electrolytes, in order to achieve superior fuel cell performance at lower temperature range.

#### 4.3. Cell Geometry and Microstructure Optimisation

The present-day materials for constructing SOFCs remains virtually the same for the past years as only few numbers of suitable materials could be applied due to high operating temperatures. Having been aware of this constraint, an approach to realising high-performance SOFCs is by refining cell geometry, associated with microstructural design and optimisation. An appropriate microstructure design could be beneficial to improve the stability of Ni-based anodes with regard to the carbon formation so as to come up with a reliable fuel cell that offers stable conversion performance. The microstructure of a cell plays an important role, particularly during the transport of gases to and from the TPB region which influences the concentration polarisation. Most common geometries for an SOFC are flat and tubular, wherein similar preparation techniques to those described in the literature are still being used, including screen printing and tape casting. A newer design, microtubular cell has been introduced in the 1990s [187] which presents extra benefits which include smaller and portable size for easy transportation, rapid start-up and shutdown, better thermal shock resistance and improved volumetric power density.

There are basically two ways to produce microtubes: plastic mass ram extrusion and the phase inversion-assisted extrusion method (also known as a spinning process) [188]. Contrary to ram-extrusion-based methods, the latter could form microtubes having distinctive microstructure due to the controllability and flexibility of the process. The microtubes derived from the phase-inversion method typically has a plurality of self-organised microchannels in the cross section of the microtube walls and sponge-like structure. The presence of the former has been described to facilitate gas transport, whereas the latter provides mechanical robustness.

The main advantage of the phase inversion method is better microstructural designing, which could be tailored by adjusting the spinning parameters and the sintering step. More interestingly, such technique also allows the fabrication of multichannel microtube [189–191] and multilayer microtubes, up to three layers in a single step [135,182,192,193]. The unique structure of the microtubular SOFCs developed from such technique have demonstrated excellent electrochemical performance [192,194]. Ni-based anode-supported microtubes derived from the phase-inversion process has a common asymmetric structure, whereby such microtubular cells developed using this method have presented outstanding electrochemical performance for operation with H<sub>2</sub> [135,195–197].

A proof-of-concept study by Lee et al. showed that various ceramic microtube designs could be derived using a phase inversion method [198]. This includes microtubes having microchannels with open entrances that could act as a substrate for catalyst deposition, which could later be developed as SOFCs with enhanced properties. If such tubes are

derived using electrolyte materials, they can act as an appropriate scaffold for anode material addition, which require less amount to be added compared to the conventional anode–suspension mixture. For instance, YSZ microtube with open entrances which suitable functioned as a scaffold for Cu–CeO<sub>2</sub> impregnation has been successfully developed and presented good performance under direct methane–fuel cell mode [176].

More interestingly, the success in producing microtubes with multichannel design or so-called micromonolithic could help to address issues regarding the mechanical stability of the microtubes which appears to be a major impediment from commercialisation. Recent development of multichannel microtubular SOFCs, otherwise known as micromonolithic cells has shown excellent fuel cell performance under H<sub>2</sub>-fuelled system [190,191,199,200] and low-calorific CH<sub>4</sub>-fuelled operation, respectively [64]. Nevertheless, more work can be conducted to further improve not only the microstructure of the microtubular cell but also to bundle the microtubes together to obtain larger power output.

#### *4.4. Key Factors Influencing the Efficiency of Hydrocarbon-Fuelled SOFCs*

Despite the promising prospects of applying hydrocarbons as fuel for SOFCs, it remains crucial to identify the various factors that impact the efficiency of the system. This recognition is vital for advancing the technology, optimising its performance and ensuring its successful integration into the energy landscape. Among the key factors that affect cell efficiency is the fuel composition and quality. While numerous studies to date are conducted at a laboratory scale using pure hydrocarbons, the actual composition and quality of hydrocarbon fuels (i.e., natural gas or biogas) to be applied in SOFCs will exert a considerable impact on cell efficiency. Impurities present in the fuel, such as sulphur and heavy metals, can poison the catalysts used in the fuel cell's anodes. This poisoning effect can degrade the performance of the anodes, leading to poor electrochemical reactions and reduced overall efficiency. In addition, impurities can also lead to carbon deposition, where unconverted hydrocarbons form solid carbon deposits on the anodes. These deposits can block active anode sites, increase overpotentials (i.e., energy losses) and reduce the cell's efficiency. Variations in the hydrocarbon mixture alter the kinetics of the reforming reactions, which are responsible for converting hydrocarbons into H<sub>2</sub>-rich gases. These as well will negatively impact the fuel conversion, thereby reducing the overall effectiveness of the cell.

In addition, the efficiency of hydrocarbon conversion within SOFCs relies on the kinetics of reforming reactions, which transform hydrocarbons into H<sub>2</sub>-rich gases. The choice of catalysts and their properties (i.e., activity and stability) significantly influence the extent of hydrocarbon conversion. Catalysts have a critical role in accelerating these reactions and facilitating the production of H<sub>2</sub>, a vital reactant in the electrochemical reactions taking place within the cell. Efficient reforming reactions are crucial as they ensure a continuous supply of H<sub>2</sub> for the electrochemical processes, thus enhancing the overall efficiency of the fuel cell. Catalyst degradation over time can lead to reduced reforming effectiveness and, subsequently, a decline in the cell's performance.

Operating temperature is another factor affecting SOFCs efficiency. Higher temperatures can improve the kinetics of both electrochemical reactions and fuel reforming. Elevated temperatures increase the speed upon which reactions occur, hence promoting more efficient energy conversion. Better reforming kinetics led to improved H<sub>2</sub> production, while faster electrochemical reactions result in higher power output. However, maintaining high temperatures poses challenges such as thermal management and material compatibility. Excessive heat can lead to material degradation, impacting the longevity and stability of the cell. Therefore, balancing the benefits of improved kinetics with the challenges of high-temperature operation is decisive for achieving optimum efficiency.

Overall, understanding and optimising the critical factors influencing hydrocarbon-fuelled SOFCs is pivotal. This knowledge allows researchers and engineers to continuously improve the cell and system design, addressing challenges in fuel composition, operating temperature and materials selection for better efficiency and performance. Effective

management of fuel impurities, proper material selection and precise temperature control contribute to SOFC durability, while enhanced efficiency leads to reduced fuel consumption, lower emissions and potential economic benefits. An SOFC is thus holds promise for a cleaner energy future and increased competitiveness in energy systems.

## 5. Conclusions

A major societal goal is clean and efficient energy generation technology using renewable sources, combined with the minimisation of the emission of both atmospheric pollutants and greenhouse gases. SOFC technology emerges as a promising way to produce clean energy to replace conventional combustion techniques in high efficiency. This relatively new technology is typically operated with hydrogen ( $H_2$ ). However, a major drawback of the  $H_2$ -fuelled system is that  $H_2$  is expensive, with most of it being produced from natural gas steam reforming processes. In addition, energy requirements are not satisfactorily effective to generate  $H_2$  in a cost-efficient way. Therefore, with SOFCs, the direct use of hydrocarbons as fuel without first externally reforming them to  $H_2$  will significantly decrease the complexity and cost of a fuel cell system. There are various approaches to direct hydrocarbon utilisation described in this review highlighting the internal reforming process and the direct feeding of pure fuel to the system. This allows the exclusion of an external reformer and circumvents the requirement for the complicated water and heat exchange system necessary to reform hydrocarbons before entering the anode compartment.

The literature shows that the direct use of hydrocarbon fuel for SOFCs is promising if certain precautions and strategies are to be applied. In comparison,  $CH_4$ -fuelled SOFCs are well-studied as it poses lesser challenges compared to heavier hydrocarbons. Regardless of the fuel types, the target of most studies largely focused on the effects of catalyst compositions, modifications and reaction conditions toward achieving high conversion and selectivity. Finding the appropriate anode materials with excellent performance and sufficient robustness is difficult due to challenging operating conditions. Thus, continuous efforts have been made to reduce working temperatures to allow more materials to be considered with better electrochemical performance.

The SOFC technology has been developed with research aiming at utilising fuel directly both with and without internal reforming and preferably at lower operating temperatures. This includes the development of alternative anode materials (i.e., non-Ni-based anodes) that can tolerate, if not completely eliminate, carbon formation while remaining stable upon exposure to other contaminants (such as  $H_2S$ ). Use of perovskites as the cell materials could lead to the reduced operating temperature, but challenges persist with hydrocarbon as fuels due to high anode polarisation resistance. Lowering the anodic activation overpotentials along with optimising and maintaining the microstructure remains as critical aspects to be addressed for success in this field. While more investigation is needed, the future looks promising for the commercialisation of direct hydrocarbon SOFCs.

**Author Contributions:** Conceptualization, M.F.R.; investigation, M.F.R., T.L., M.H.D.O. and K.L.; resources, M.F.R. and K.L.; writing—original draft preparation, M.F.R.; writing—review and editing, M.F.R., T.L., M.H.D.O., F.H.A. and K.L.; visualization, M.F.R. and F.H.A.; supervision, T.L. and K.L. All authors have read and agreed to the published version of the manuscript.

**Funding:** M.F.R. would like to acknowledge the Universiti Malaya-Research University Grant (GPF059B-2020) for funding this research. This study was also supported in part by the SATU Joint Research Scheme (JRS) (ST045-2022).

**Data Availability Statement:** Not applicable.

**Conflicts of Interest:** The authors declare no conflict of interest.



## References

1. Kirubakaran, A.; Jain, S.; Nema, R.K. A review on fuel cell technologies and power electronic interface. *Renew. Sustain. Energy Rev.* **2009**, *13*, 2430–2440. [[CrossRef](#)]
2. Mekhilef, S.; Saidur, R.; Safari, A. Comparative study of different fuel cell technologies. *Renew. Sustain. Energy Rev.* **2012**, *16*, 981–989. [[CrossRef](#)]
3. Giddey, S.; Badwal, S.P.S.; Kulkarni, A.; Munnings, C. A comprehensive review of direct carbon fuel cell technology. *Prog. Energy Combust. Sci.* **2012**, *38*, 360–399. [[CrossRef](#)]
4. Wang, Y.; Chen, K.S.; Mishler, J.; Cho, S.C.; Adroher, X.C. A review of polymer electrolyte membrane fuel cells: Technology, applications, and needs on fundamental research. *Appl. Energy* **2011**, *88*, 981–1007. [[CrossRef](#)]
5. Peighambaroust, S.J.; Rowshanzamir, S.; Amjadi, M. Review of the proton exchange membranes for fuel cell applications. *Int. J. Hydrogen Energy* **2010**, *35*, 9349–9384. [[CrossRef](#)]
6. Boudghene Stambouli, A.; Traversa, E. Fuel cells, an alternative to standard sources of energy. *Renew. Sustain. Energy Rev.* **2002**, *6*, 295–304. [[CrossRef](#)]
7. Brandon, N.P.; Skinner, S.; Steele, B.C.H. Recent Advances in Materials for Fuel Cells. *Annu. Rev. Mater. Res.* **2003**, *33*, 183–213. [[CrossRef](#)]
8. Su, H.; Hu, Y.H. Progress in low-temperature solid oxide fuel cells with hydrocarbon fuels. *Chem. Eng. J.* **2020**, *402*, 126235. [[CrossRef](#)]
9. Liu, F.; Duan, C. Direct-Hydrocarbon Proton-Conducting Solid Oxide Fuel Cells. *Sustainability* **2021**, *13*, 4736. [[CrossRef](#)]
10. Zarabi Golkhatmi, S.; Asghar, M.I.; Lund, P.D. A review on solid oxide fuel cell durability: Latest progress, mechanisms, and study tools. *Renew. Sustain. Energy Rev.* **2022**, *161*, 112339. [[CrossRef](#)]
11. McIntosh, S.; He, H.; Lee, S.I.; Costa-Nunes, O.; Krishnan, V.V.; Vohs, J.M.; Gorte, R.J. An Examination of Carbonaceous Deposits in Direct-Utilization SOFC Anodes. *J. Electrochem. Soc.* **2004**, *151*, A604–A608. [[CrossRef](#)]
12. Sun, C.; Stimming, U. Recent anode advances in solid oxide fuel cells. *J. Power Sources* **2007**, *171*, 247–260. [[CrossRef](#)]
13. Shi, N.; Xie, Y.; Yang, Y.; Xue, S.; Li, X.; Zhu, K.; Huan, D.; Peng, R.; Xia, C.; Lu, Y. Review of anodic reactions in hydrocarbon fueled solid oxide fuel cells and strategies to improve anode performance and stability. *Mater. Renew. Sustain. Energy* **2020**, *9*, 6. [[CrossRef](#)]
14. Shabri, H.A.; Othman, M.H.D.; Mohamed, M.A.; Kurniawan, T.A.; Jamil, S.M. Recent progress in metal-ceramic anode of solid oxide fuel cell for direct hydrocarbon fuel utilization: A review. *Fuel Process. Technol.* **2021**, *212*, 106626. [[CrossRef](#)]
15. Duan, C.; Kee, R.J.; Zhu, H.; Karakaya, C.; Chen, Y.; Ricote, S.; Jarry, A.; Crumlin, E.J.; Hook, D.; Braun, R.; et al. Highly durable, coking and sulfur tolerant, fuel-flexible protonic ceramic fuel cells. *Nature* **2018**, *557*, 217–222. [[CrossRef](#)]
16. Zhang, W.; Hu, Y.H. Progress in proton-conducting oxides as electrolytes for low-temperature solid oxide fuel cells: From materials to devices. *Energy Sci. Eng.* **2021**, *9*, 984–1011. [[CrossRef](#)]
17. Mojaver, P.; Chitsaz, A.; Sadeghi, M.; Khalilarya, S. Comprehensive comparison of SOFCs with proton-conducting electrolyte and oxygen ion-conducting electrolyte: Thermoeconomic analysis and multi-objective optimization. *Energy Convers. Manag.* **2020**, *205*, 112455. [[CrossRef](#)]
18. Atkinson, A.; Barnett, S.; Gorte, R.J.; Irvine, J.T.S.; McEvoy, A.J.; Mogensen, M.; Singhal, S.C.; Vohs, J. Advanced anodes for high-temperature fuel cells. *Nat. Mater.* **2004**, *3*, 17–27. [[CrossRef](#)]
19. Mogensen, M.; Kammer, K. Conversion of hydrocarbons in solid oxide fuel cells. *Annu. Rev. Mater. Res.* **2003**, *33*, 321–331. [[CrossRef](#)]
20. Gorte, R.; McIntosh, S. Direct Hydrocarbon Solid Oxide Fuel Cells. *Chem. Rev.* **2004**, *104*, 4845–4866.
21. Chen, T.; Wang, W.G.; Miao, H.; Li, T.; Xu, C. Evaluation of carbon deposition behavior on the nickel/yttrium-stabilized zirconia anode-supported fuel cell fueled with simulated syngas. *J. Power Sources* **2011**, *196*, 2461–2468. [[CrossRef](#)]
22. Hanna, J.; Lee, W.Y.; Shi, Y.; Ghoniem, A.F. Fundamentals of electro- and thermochemistry in the anode of solid-oxide fuel cells with hydrocarbon and syngas fuels. *Prog. Energy Combust. Sci.* **2014**, *40*, 74–111. [[CrossRef](#)]
23. Dokmaingam, P.; Irvine, J.T.S.; Assabumrungrat, S.; Charojrochkul, S.; Laosiripojana, N. Modeling of IT-SOFC with indirect internal reforming operation fueled by methane: Effect of oxygen adding as autothermal reforming. *Int. J. Hydrogen Energy* **2010**, *35*, 13271–13279. [[CrossRef](#)]
24. Aguiar, P.; Chadwick, D.; Kershenbaum, L. Modelling of an indirect internal reforming solid oxide fuel cell. *Chem. Eng. Sci.* **2002**, *57*, 1665–1677. [[CrossRef](#)]
25. Marina, O.A.; Mogensen, M. High-temperature conversion of methane on a composite gadolinia-doped ceria–gold electrode. *Appl. Catal. A Gen.* **1999**, *189*, 117–126. [[CrossRef](#)]
26. Park, S.; Vohs, J.M.; Gorte, R.J. Direct oxidation of hydrocarbons in a solid-oxide fuel cell. *Nature* **2000**, *404*, 265–267. [[CrossRef](#)]
27. Shin, T.H.; Ida, S.; Ishihara, T. Doped CeO<sub>2</sub>–LaFeO<sub>3</sub> Composite Oxide as an Active Anode for Direct Hydrocarbon-Type Solid Oxide Fuel Cells. *J. Am. Chem. Soc.* **2011**, *133*, 19399–19407. [[CrossRef](#)] [[PubMed](#)]
28. Zha, S.; Cheng, Z.; Liu, M. Sulfur Poisoning and Regeneration of Ni-Based Anodes in Solid Oxide Fuel Cells. *J. Electrochem. Soc.* **2007**, *154*, B201–B206. [[CrossRef](#)]

29. Niakolas, D.K. Sulfur poisoning of Ni-based anodes for Solid Oxide Fuel Cells in H/C-based fuels. *Appl. Catal. A Gen.* **2014**, *486*, 123–142. [[CrossRef](#)]
30. Sperle, T.; Chen, D.; Lødeng, R.; Holmen, A. Pre-reforming of natural gas on a Ni catalyst: Criteria for carbon free operation. *Appl. Catal. A Gen.* **2005**, *282*, 195–204. [[CrossRef](#)]
31. Kee, R.J.; Zhu, H.; Sukeshini, A.M.; Jackson, G.S. Solid Oxide Fuel Cells: Operating Principles, Current Challenges, and the Role of Syngas. *Combust. Sci. Technol.* **2008**, *180*, 1207–1244. [[CrossRef](#)]
32. Sasaki, K.; Teraoka, Y. Equilibria in Fuel Cell Gases: II. The C-H-O Ternary Diagrams. *J. Electrochem. Soc.* **2003**, *150*, A885–A888. [[CrossRef](#)]
33. Offer, G.J.; Mermelstein, J.; Brightman, E.; Brandon, N.P. Thermodynamics and Kinetics of the Interaction of Carbon and Sulfur with Solid Oxide fuel Cell Anodes. *J. Am. Ceram. Soc.* **2009**, *92*, 763–780. [[CrossRef](#)]
34. Ivers-Tiffée, E.; Timmermann, H.; Leonide, A.; Menzler, N.H.; Malzbender, J. Methane reforming kinetics, carbon deposition, and redox durability of Ni/8 yttria-stabilized zirconia (YSZ) anodes. In *Handbook of Fuel Cells*; John Wiley & Sons, Ltd.: Hoboken, NJ, USA, 2010.
35. Tang, P.; Zhu, Q.; Wu, Z.; Ma, D. Methane activation: The past and future. *Energy Environ. Sci.* **2014**, *7*, 2580–2591. [[CrossRef](#)]
36. Murray, E.P.; Tsai, T.; Barnett, S.A. A direct-methane fuel cell with a ceria-based anode. *Nature* **1999**, *400*, 649–651. [[CrossRef](#)]
37. Hibino, T.; Hashimoto, A.; Asano, K.; Yano, M.; Suzuki, M.; Sanob, M. An Intermediate-Temperature Solid Oxide Fuel Cell Providing Higher Performance with Hydrocarbons than with Hydrogen. *Electrochem Solid-State Lett.* **2002**, *5*, A242–A244. [[CrossRef](#)]
38. Koh, J.-H.; Yoo, Y.-S.; Park, J.-W.; Lim, H.C. Carbon deposition and cell performance of Ni-YSZ anode support SOFC with methane fuel. *Solid State Ion.* **2002**, *149*, 157–166. [[CrossRef](#)]
39. Kim, H.; Lu, C.; Worrell, W.L.; Vohs, J.M.; Gorte, R.J. Cu-Ni Cermet Anodes for Direct Oxidation of Methane in Solid-Oxide Fuel Cells. *J. Electrochem. Soc.* **2002**, *149*, A247. [[CrossRef](#)]
40. Gorte, R.; Vohs, J.; Kim, H. Novel SOFC anodes for the direct electrochemical oxidation of hydrocarbon. *J. Power Sources* **2002**, *106*, 10–15. [[CrossRef](#)]
41. Hibino, T.; Hashimoto, A.; Yano, M.; Suzuki, M.; Sano, M. Ru-catalyzed anode materials for direct hydrocarbon SOFCs. *Electrochim. Acta* **2003**, *48*, 2531–2537. [[CrossRef](#)]
42. Liu, J.; Barnett, S.A. Operation of anode-supported solid oxide fuel cells on methane and natural gas. *Solid State Ion.* **2003**, *158*, 11–16. [[CrossRef](#)]
43. Lin, Y.; Zhan, Z.; Liu, J.; Barnett, S.A. Direct operation of solid oxide fuel cells with methane fuel. *Solid State Ion.* **2005**, *176*, 1827–1835. [[CrossRef](#)]
44. Li, S.; Wang, S.; Nie, H.; Wen, T.-I. A direct-methane solid oxide fuel cell with a double-layer anode. *J. Solid State Electrochem.* **2005**, *11*, 59–64. [[CrossRef](#)]
45. Zhu, W.; Xia, C.; Fan, J.; Peng, R.; Meng, G. Ceria coated Ni as anodes for direct utilization of methane in low-temperature solid oxide fuel cells. *J. Power Sources* **2006**, *160*, 897–902. [[CrossRef](#)]
46. Shao, Z.; Mederos, J.; Chueh, W.C.; Haile, S.M. High power-density single-chamber fuel cells operated on methane. *J. Power Sources* **2006**, *162*, 589–596. [[CrossRef](#)]
47. Klein, J.-M.; Hénault, M.; Gélin, P.; Bultel, Y.; Georges, S. A Solid Oxide Fuel Cell Operating in Gradual Internal Reforming Conditions under Pure Dry Methane. *Electrochem. Solid-State Lett.* **2008**, *11*, B144–B147. [[CrossRef](#)]
48. Akhtar, N.; Decent, S.P.; Loghini, D.; Kendall, K. Mixed-reactant, micro-tubular solid oxide fuel cells: An experimental study. *J. Power Sources* **2009**, *193*, 39–48. [[CrossRef](#)]
49. Akhtar, N.; Decent, S.P.; Kendall, K. Cell temperature measurements in micro-tubular, single-chamber, solid oxide fuel cells (MT-SC-SOFCs). *J. Power Sources* **2010**, *195*, 7818–7824. [[CrossRef](#)]
50. Kan, H.; Lee, H. Enhanced stability of Ni-Fe/GDC solid oxide fuel cell anodes for dry methane fuel. *Catal. Commun.* **2010**, *12*, 36–39. [[CrossRef](#)]
51. Akhtar, N.; Kendall, K. Silver modified cathode for a micro-tubular, single-chamber solid oxide fuel cell. *Int. J. Hydrogen Energy* **2011**, *36*, 773–778. [[CrossRef](#)]
52. Suzuki, T.; Yamaguchi, T.; Hamamoto, K.; Fujishiro, Y.; Awano, M.; Sammes, N. A functional layer for direct use of hydrocarbon fuel in low temperature solid-oxide fuel cells. *Energy Environ. Sci.* **2011**, *4*, 940–943. [[CrossRef](#)]
53. Calise, F.; Restuccia, G.; Sammes, N. Experimental analysis of performance degradation of micro-tubular solid oxide fuel cells fed by different fuel mixtures. *J. Power Sources* **2011**, *196*, 301–312. [[CrossRef](#)]
54. Shao, Z.; Zhang, C.; Wang, W.; Su, C.; Zhou, W.; Zhu, Z.; Park, H.J.; Kwak, C. Electric Power and Synthesis Gas Co-generation From Methane with Zero Waste Gas Emission. *Angew. Chem. Int. Ed.* **2011**, *50*, 1792–1797. [[CrossRef](#)]
55. Sumi, H.; Yamaguchi, T.; Hamamoto, K.; Suzuki, T.; Fujishiro, Y. Impact of direct butane microtubular solid oxide fuel cells. *J. Power Sources* **2012**, *220*, 74–78. [[CrossRef](#)]
56. Meng, X.; Gong, X.; Yin, Y.; Yang, N.; Tan, X.; Ma, Z.-F. Effect of the co-spun anode functional layer on the performance of the direct-methane microtubular solid oxide fuel cells. *J. Power Sources* **2014**, *247*, 587–593. [[CrossRef](#)]

57. Yoon, D.; Manthiram, A. Hydrocarbon-fueled solid oxide fuel cells with surface-modified, hydroxylated Sn/Ni-Ce<sub>0.8</sub>Gd<sub>0.2</sub>O<sub>1.9</sub> heterogeneous catalyst anode. *J. Mater. Chem. A* **2014**, *2*, 17041–17046. [[CrossRef](#)]
58. Ma, J.; Jiang, C.; Connor, P.A.; Cassidy, M.; Irvine, J.T.S. Highly efficient, coking-resistant SOFCs for energy conversion using biogas fuels. *J. Mater. Chem. A* **2015**, *3*, 19068–19076. [[CrossRef](#)]
59. Liu, L.; Yang, Q.; Yang, W.; Qi, X.; Sun, C.; Chen, L. Li/Na Modified Ni-SDC Anode for Methane-Fueled Solid Oxide Fuel Cells. *ECS Trans.* **2015**, *68*, 1403–1409. [[CrossRef](#)]
60. Majewski, A.J.; Dhir, A. Direct Utilization of Methane in Microtubular-SOFC. *ECS Trans.* **2015**, *68*, 2189–2198. [[CrossRef](#)]
61. Konwar, D.; Yoon, H.H. A methane-fueled SOFC based on a thin BaZr<sub>0.1</sub>Ce<sub>0.7</sub>Y<sub>0.1</sub>Yb<sub>0.1</sub>O<sub>3-δ</sub> electrolyte film and a LaNi<sub>0.6</sub>Co<sub>0.4</sub>O<sub>3</sub> anode functional layer. *J. Mater. Chem. A* **2016**, *4*, 5102–5106. [[CrossRef](#)]
62. Hua, B.; Yan, N.; Li, M.; Sun, Y.-F.; Zhang, Y.-Q.; Li, J.; Etsell, T.; Sarkar, P.; Luo, J.-L. Anode-Engineered Protonic Ceramic Fuel Cell with Excellent Performance and Fuel Compatibility. *Adv. Mater.* **2016**, *28*, 8922–8926. [[CrossRef](#)] [[PubMed](#)]
63. Zhao, J.; Xu, X.; Zhou, W.; Blakey, I.; Liu, S.; Zhu, Z. Proton-Conducting La-Doped Ceria-Based Internal Reforming Layer for Direct Methane Solid Oxide Fuel Cells. *ACS Appl. Mater. Interfaces* **2017**, *9*, 33758–33765. [[CrossRef](#)]
64. Li, T.; Lu, X.; Rabuni, M.F.; Wang, B.; Farandos, N.M.; Kelsall, G.H.; Brett, D.J.L.; Shearing, P.R.; Ouyang, M.; Brandon, N.P.; et al. High-performance fuel cell designed for coking-resistance and efficient conversion of waste methane to electrical energy. *Energy Environ. Sci.* **2020**, *13*, 1879–1887. [[CrossRef](#)]
65. Yuan, X.; Chen, H.; Tian, W.; Shi, J.; Zhou, W.; Cheng, F.; Li, S.-D.; Shao, Z. Utilization of low-concentration coal-bed gas to generate power using a core-shell catalyst-modified solid oxide fuel cell. *Renew. Energy* **2020**, *147*, 602–609. [[CrossRef](#)]
66. Bierschenk, D.M.; Pillai, M.R.; Lin, Y.; Barnett, S.A. Effect of Ethane and Propane in Simulated Natural Gas on the Operation of Ni-YSZ Anode Supported Solid Oxide Fuel Cells. *Fuel Cells* **2010**, *10*, 1129–1134. [[CrossRef](#)]
67. Peters, R.; Riensche, E.; Cremer, P. Pre-reforming of natural gas in solid oxide fuel-cell systems. *J. Power Sources* **2000**, *86*, 432–441. [[CrossRef](#)]
68. Fan, L.; Li, C.E.; Aravind, P.V.; Cai, W.; Han, M.; Brandon, N. Methane reforming in solid oxide fuel cells: Challenges and strategies. *J. Power Sources* **2022**, *538*, 231573. [[CrossRef](#)]
69. Weissbart, J.; Ruka, R. A Solid Electrolyte Fuel Cell. *J. Electrochem. Soc.* **1962**, *109*, 723–726. [[CrossRef](#)]
70. Liese, E.A.; Gemmen, R.S. Performance Comparison of Internal Reforming Against External Reforming in a Solid Oxide Fuel Cell, Gas Turbine Hybrid System. *J. Eng. Gas Turbines Power* **2005**, *127*, 86–90. [[CrossRef](#)]
71. Timmermann, H.; Fouquet, D.; Weber, A.; Ivers-Tiffée, E.; Hennings, U.; Reimert, R. Internal Reforming of Methane at Ni/YSZ and Ni/CGO SOFC Cermet Anodes. *Fuel Cells* **2006**, *6*, 307–313. [[CrossRef](#)]
72. Nakagawa, N.; Sagara, H.; Kato, K. Catalytic activity of Ni-YSZ-CeO<sub>2</sub> anode for the steam reforming of methane in a direct internal-reforming solid oxide fuel cell. *J. Power Sources* **2001**, *92*, 88–94. [[CrossRef](#)]
73. Finnerty, C.M.; Coe, N.J.; Cunningham, R.H.; Ormerod, R.M. Carbon formation on and deactivation of nickel-based/zirconia anodes in solid oxide fuel cells running on methane. *Catal. Today* **1998**, *46*, 137–145. [[CrossRef](#)]
74. Eguchi, K.; Kojo, H.; Takeguchi, T.; Kikuchi, R.; Sasaki, K. Fuel flexibility in power generation by solid oxide fuel cells. *Solid State Ion.* **2002**, *152–153*, 411–416. [[CrossRef](#)]
75. Tavares, A.C.; Kuzin, B.L.; Beresnev, S.M.; Bogdanovich, N.M.; Kurumchin, E.K.; Dubitsky, Y.A.; Zaopo, A. Novel copper-based anodes for solid oxide fuel cells with samaria-doped ceria electrolyte. *J. Power Sources* **2008**, *183*, 20–25. [[CrossRef](#)]
76. Takeguchi, T.; Kani, Y.; Yano, T.; Kikuchi, R.; Eguchi, K.; Tsujimoto, K.; Uchida, Y.; Ueno, A.; Omoshiki, K.; Aizawa, M. Study on steam reforming of CH<sub>4</sub> and C<sub>2</sub> hydrocarbons and carbon deposition on Ni-YSZ cermets. *J. Power Sources* **2002**, *112*, 588–595. [[CrossRef](#)]
77. Takeguchi, T.; Kikuchi, R.; Yano, T.; Eguchi, K.; Murata, K. Effect of precious metal addition to Ni-YSZ cermet on reforming of CH<sub>4</sub> and electrochemical activity as SOFC anode. *Catal. Today* **2003**, *84*, 217–222. [[CrossRef](#)]
78. Hua, B.; Li, M.; Zhang, W.; Pu, J.; Chi, B.; Jian, L. Methane On-Cell Reforming by Alloys Reduced from Ni<sub>0.5</sub>Cu<sub>0.5</sub>Fe<sub>2</sub>O<sub>4</sub> for Direct-Hydrocarbon Solid Oxide Fuel Cells. *J. Electrochem. Soc.* **2014**, *161*, F569–F575. [[CrossRef](#)]
79. Nikooyeh, K.; Jeje, A.A.; Hill, J.M. 3D modeling of anode-supported planar SOFC with internal reforming of methane. *J. Power Sources* **2007**, *171*, 601–609. [[CrossRef](#)]
80. Mogensen, D.; Grunwaldt, J.D.; Hendriksen, P.V.; Dam-Johansen, K.; Nielsen, J.U. Internal steam reforming in solid oxide fuel cells: Status and opportunities of kinetic studies and their impact on modelling. *J. Power Sources* **2011**, *196*, 25–38. [[CrossRef](#)]
81. Kim, T.; Moon, S.; Hong, S.-I. Internal carbon dioxide reforming by methane over Ni-YSZ-CeO<sub>2</sub> catalyst electrode in electrochemical cell. *Appl. Catal. A Gen.* **2002**, *224*, 111–120. [[CrossRef](#)]
82. Barelli, L.; Ottaviano, A. Solid oxide fuel cell technology coupled with methane dry reforming: A viable option for high efficiency plant with reduced CO<sub>2</sub> emissions. *Energy* **2014**, *71*, 118–129. [[CrossRef](#)]
83. Aw, M.S.; Zorko, M.; Osojnik Črnivec, I.G.; Pintar, A. Progress in the Synthesis of Catalyst Supports: Synergistic Effects of Nanocomposites for Attaining Long-Term Stable Activity in CH<sub>4</sub>-CO<sub>2</sub> Dry Reforming. *Ind. Eng. Chem. Res.* **2015**, *54*, 3775–3787. [[CrossRef](#)]
84. Fonseca, R.O.D.; Silva, A.A.A.D.; Signorelli, M.R.M.; Rabelo-Neto, R.C.; Noronha, F.B.; Simões, R.C.C.; Mattos, L.V. Nickel/Doped Ceria Solid Oxide Fuel Cell Anodes for Dry Reforming of Methane. *J. Braz. Chem. Soc.* **2014**, *25*, 2356–2363. [[CrossRef](#)]

85. Fukuhara, C.; Hyodo, R.; Yamamoto, K.; Masuda, K.; Watanabe, R. A novel nickel-based catalyst for methane dry reforming: A metal honeycomb-type catalyst prepared by sol-gel method and electroless plating. *Appl. Catal. A Gen.* **2013**, *468*, 18–25. [[CrossRef](#)]
86. Bobrova, L.N.; Bobin, A.S.; Mezentseva, N.V.; Sadykov, V.A.; Thybaut, J.W.; Marin, G.B. Kinetic assessment of dry reforming of methane on Pt + Ni containing composite of fluorite-like structure. *Appl. Catal. B Environ.* **2016**, *182*, 513–524. [[CrossRef](#)]
87. Smirnova, A.; Sadykov, V.; Mezentseva, N.; Bunina, R.; Pilipenko, V.V.; Alikina, G.; Krieger, T.A.; Bobrova, L.N.; Smorygo, O.L.; Van Berkel, F.; et al. Design and Testing of Structured Catalysts for Internal Reforming of CH<sub>4</sub> in Intermediate Temperature Solid Oxide Fuel Cells (IT SOFC). *ECS Trans.* **2011**, *35*, 2771–2780. [[CrossRef](#)]
88. Pakhare, D.; Spivey, J. A review of dry (CO<sub>2</sub>) reforming of methane over noble metal catalysts. *Chem. Soc. Rev.* **2014**, *43*, 7813–7837. [[CrossRef](#)]
89. Lanzini, A.; Guerra, C.; Leone, P.; Santarelli, M.; Smeacetto, F.; Fiorilli, S.; Gondolini, A.; Mercadelli, E.; Sanson, A.; Brandon, N.P. Influence of the microstructure on the catalytic properties of SOFC anodes under dry reforming of methane. *Mater. Lett.* **2016**, *164*, 312–315. [[CrossRef](#)]
90. Hua, B.; Yan, N.; Li, M.; Zhang, Y.-Q.; Sun, Y.-F.; Li, J.; Etsell, T.; Sarkar, P.; Chuang, K.; Luo, J.-L. Novel layered solid oxide fuel cells with multiple-twinned Ni<sub>0.8</sub>Co<sub>0.2</sub> nanoparticles: The key to thermally independent CO<sub>2</sub> utilization and power-chemical cogeneration. *Energy Environ. Sci.* **2016**, *9*, 207–215. [[CrossRef](#)]
91. Lanzini, A.; Leone, P.; Guerra, C.; Smeacetto, F.; Brandon, N.P.; Santarelli, M. Durability of anode supported Solid Oxide Fuel Cells (SOFC) under direct dry-reforming of methane. *Chem. Eng. J.* **2013**, *220* (Suppl. C), 254–263. [[CrossRef](#)]
92. Assabumrungrat, S.; Laosiripojana, N.; Piroonlerkgul, P. Determination of the boundary of carbon formation for dry reforming of methane in a solid oxide fuel cell. *J. Power Sources* **2006**, *159*, 1274–1282. [[CrossRef](#)]
93. Pillai, M.; Bierschenk, D.; Barnett, S. Electrochemical Partial Oxidation of Methane in Solid Oxide Fuel Cells: Effect of Anode Reforming Activity. *Catal. Lett.* **2008**, *121*, 19–23. [[CrossRef](#)]
94. Zhu, H.; Kee, R.J.; Pillai, M.R.; Barnett, S.A. Modeling electrochemical partial oxidation of methane for cogeneration of electricity and syngas in solid-oxide fuel cells. *J. Power Sources* **2008**, *183*, 143–150. [[CrossRef](#)]
95. Liso, V.; Olesen, A.C.; Nielsen, M.P.; Kær, S.K. Performance comparison between partial oxidation and methane steam reforming processes for solid oxide fuel cell (SOFC) micro combined heat and power (CHP) system. *Energy* **2011**, *36*, 4216–4226. [[CrossRef](#)]
96. Timmermann, H.; Sawady, W.; Reimert, R.; Ivers-Tiffée, E. Kinetics of (reversible) internal reforming of methane in solid oxide fuel cells under stationary and APU conditions. *J. Power Sources* **2010**, *195*, 214–222. [[CrossRef](#)]
97. Asano, K.; Hibino, T.; Iwahara, H. A Novel Solid Oxide Fuel Cell System Using the Partial Oxidation of Methane. *J. Electrochem. Soc.* **1995**, *142*, 3241–3245. [[CrossRef](#)]
98. Christian Enger, B.; Lødeng, R.; Holmen, A. A review of catalytic partial oxidation of methane to synthesis gas with emphasis on reaction mechanisms over transition metal catalysts. *Appl. Catal. A Gen.* **2008**, *346*, 1–27. [[CrossRef](#)]
99. Velasco, J.A.; Fernandez, C.; Lopez, L.; Cabrera, S.; Boutonnet, M.; Järås, S. Catalytic partial oxidation of methane over nickel and ruthenium based catalysts under low O<sub>2</sub>/CH<sub>4</sub> ratios and with addition of steam. *Fuel* **2015**, *153*, 192–201. [[CrossRef](#)]
100. Lyubovskiy, M.; Roychoudhury, S.; LaPierre, R. Catalytic partial “oxidation of methane to syngas” at elevated pressures. *Catal. Lett.* **2005**, *99*, 113–117. [[CrossRef](#)]
101. Enger, B.C.; Lødeng, R.; Holmen, A. Evaluation of reactor and catalyst performance in methane partial oxidation over modified nickel catalysts. *Appl. Catal. A Gen.* **2009**, *364*, 15–26. [[CrossRef](#)]
102. Cheekatamarla, P.K.; Finnerty, C.M.; Cai, J. Internal reforming of hydrocarbon fuels in tubular solid oxide fuel cells. *Int. J. Hydrogen Energy* **2008**, *33*, 1853–1858. [[CrossRef](#)]
103. Majewski, A.J.; Dhir, A. Direct Utilization of Methane in Microtubular-SOFC. *J. Electrochem. Soc.* **2016**, *163*, F272–F277. [[CrossRef](#)]
104. Lee, D.; Myung, J.; Tan, J.; Hyun, S.-H.; Irvine, J.T.S.; Kim, J.; Moon, J. Direct methane solid oxide fuel cells based on catalytic partial oxidation enabling complete coking tolerance of Ni-based anodes. *J. Power Sources* **2017**, *345* (Suppl. C), 30–40. [[CrossRef](#)]
105. Wang, W.; Su, C.; Wu, Y.; Ran, R.; Shao, Z. A comprehensive evaluation of a Ni–Al<sub>2</sub>O<sub>3</sub> catalyst as a functional layer of solid-oxide fuel cell anode. *J. Power Sources* **2010**, *195*, 402–411. [[CrossRef](#)]
106. Pillai, M.; Lin, Y.; Zhu, H.; Kee, R.J.; Barnett, S.A. Stability and coking of direct-methane solid oxide fuel cells: Effect of CO<sub>2</sub> and air additions. *J. Power Sources* **2010**, *195*, 271–279. [[CrossRef](#)]
107. Aslannejad, H.; Barelli, L.; Babaie, A.; Bozorgmehri, S. Effect of air addition to methane on performance stability and coking over NiO–YSZ anodes of SOFC. *Appl. Energy* **2016**, *177*, 179–186. [[CrossRef](#)]
108. Sumi, H.; Ukai, K.; Mizutani, Y.; Mori, H.; Wen, C.-J.; Takahashi, H.; Yamamoto, O. Performance of nickel–scandia-stabilized zirconia cermet anodes for SOFCs in 3% H<sub>2</sub>O–CH<sub>4</sub>. *Solid State Ion.* **2004**, *174*, 151–156. [[CrossRef](#)]
109. Klein, J.-M.; Hénault, M.; Roux, C.; Bultel, Y.; Georges, S. Direct methane solid oxide fuel cell working by gradual internal steam reforming: Analysis of operation. *J. Power Sources* **2009**, *193*, 331–337. [[CrossRef](#)]
110. Ge, X.-M.; Chan, S.-H.; Liu, Q.-L.; Sun, Q. Solid Oxide Fuel Cell Anode Materials for Direct Hydrocarbon Utilization. *Adv. Energy Mater.* **2012**, *2*, 1156–1181. [[CrossRef](#)]
111. Wang, J.B.; Jang, J.-C.; Huang, T.-J. Study of Ni-samarium-doped ceria anode for direct oxidation of methane in solid oxide fuel cells. *J. Power Sources* **2003**, *122*, 122–131. [[CrossRef](#)]
112. Sfeir, J.; Buffat, P.A.; Möckli, P.; Xanthopoulos, N.; Vasquez, R.; Joerg Mathieu, H.; Van herle, J.; Ravindranathan Thampi, K. Lanthanum Chromite Based Catalysts for Oxidation of Methane Directly on SOFC Anodes. *J. Catal.* **2001**, *202*, 229–244. [[CrossRef](#)]



113. Weber, A.; Sauer, B.; Müller, A.C.; Herbstritt, D.; Ivers-Tiffée, E. Oxidation of H<sub>2</sub>, CO and methane in SOFCs with Ni/YSZ-cermet anodes. *Solid State Ion.* **2002**, *152–153*, 543–550. [[CrossRef](#)]
114. Huang, T.-J.; Huang, M.-C. Electrochemical promotion of bulk lattice-oxygen extraction for syngas generation over Ni-GDC anodes in direct-methane SOFCs. *Chem. Eng. J.* **2008**, *135*, 216–223. [[CrossRef](#)]
115. Jiao, Y.; Zhang, L.; An, W.; Zhou, W.; Sha, Y.; Shao, Z.; Bai, J.; Li, S.-D. Controlled deposition and utilization of carbon on Ni-YSZ anodes of SOFCs operating on dry methane. *Energy* **2016**, *113*, 432–443. [[CrossRef](#)]
116. La Rosa, D.; Lo Faro, M.; Monforte, G.; Antonucci, V.; Aricò, A.S.; Sin, A. Recent Advances on the Development of NiCu Alloy Catalysts for IT-SOFCs. *ECS Trans.* **2007**, *7*, 1685–1693. [[CrossRef](#)]
117. Wang, Z.; Weng, W.; Cheng, K.; Du, P.; Shen, G.; Han, G. Catalytic modification of Ni–Sm-doped ceria anodes with copper for direct utilization of dry methane in low-temperature solid oxide fuel cells. *J. Power Sources* **2008**, *179*, 541–546. [[CrossRef](#)]
118. Liu, M.; Wang, S.; Chen, T.; Yuan, C.; Zhou, Y.; Wang, S.; Huang, J. Performance of the nano-structured Cu–Ni (alloy)–CeO<sub>2</sub> anode for solid oxide fuel cells. *J. Power Sources* **2015**, *274*, 730–735. [[CrossRef](#)]
119. Lee, S.-I.; Vohs, J.M.; Gorte, R.J. A Study of SOFC Anodes Based on Cu–Ni and Cu–Co Bimetallics in CeO<sub>2</sub>–YSZ. *J. Electrochem. Soc.* **2004**, *151*, A1319. [[CrossRef](#)]
120. Myung, J.-h.; Kim, S.-D.; Shin, T.H.; Lee, D.; Irvine, J.T.S.; Moon, J.; Hyun, S.-H. Nano-composite structural Ni–Sn alloy anodes for high performance and durability of direct methane-fueled SOFCs. *J. Mater. Chem. A* **2015**, *3*, 13801–13806. [[CrossRef](#)]
121. Yang, Q.; Chen, J.; Sun, C.; Chen, L. Direct operation of methane fueled solid oxide fuel cells with Ni cermet anode via Sn modification. *Int. J. Hydrogen Energy* **2016**, *41*, 11391–11398. [[CrossRef](#)]
122. Asamoto, M.; Miyake, S.; Sugihara, K.; Yahiro, H. Improvement of Ni/SDC anode by alkaline earth metal oxide addition for direct methane–solid oxide fuel cells. *Electrochem. Commun.* **2009**, *11*, 1508–1511. [[CrossRef](#)]
123. Serra, J.M.; Meulenberg, W.A. Thin-Film Proton BaZr<sub>0.85</sub>Y<sub>0.15</sub>O<sub>3</sub> Conducting Electrolytes: Toward an Intermediate-Temperature Solid Oxide Fuel Cell Alternative. *J. Am. Ceram. Soc.* **2007**, *90*, 2082–2089. [[CrossRef](#)]
124. Islam, S.; Hill, J.M. Barium oxide promoted Ni/YSZ solid-oxide fuel cells for direct utilization of methane. *J. Mater. Chem. A* **2014**, *2*, 1922–1929. [[CrossRef](#)]
125. Liu, Y.; Bai, Y.; Liu, J. (Ni<sub>0.75</sub>Fe<sub>0.25</sub>–xMgO)/YSZ anode for direct methane solid-oxide fuel cells. *J. Power Sources* **2011**, *196*, 9965–9969. [[CrossRef](#)]
126. Yang, Q.; Chai, F.; Ma, C.; Sun, C.; Shi, S.; Chen, L. Enhanced coking tolerance of a MgO-modified Ni cermet anode for hydrocarbon fueled solid oxide fuel cells. *J. Mater. Chem. A* **2016**, *4*, 18031–18036. [[CrossRef](#)]
127. Nabae, Y.; Yamanaka, I. Alloying effects of Pd and Ni on the catalysis of the oxidation of dry CH<sub>4</sub> in solid oxide fuel cells. *Appl. Catal. A Gen.* **2009**, *369*, 119–124. [[CrossRef](#)]
128. Babaei, A.; Jiang, S.P.; Li, J. Electrocatalytic Promotion of Palladium Nanoparticles on Hydrogen Oxidation on Ni/GDC Anodes of SOFCs via Spillover. *J. Electrochem. Soc.* **2009**, *156*, B1022–B1029. [[CrossRef](#)]
129. Shimada, H.; Takami, E.; Takizawa, K.; Hagiwara, A.; Ihara, M. Highly dispersed anodes for solid oxide fuel cells using NiO/YSZ/BZY triple-phase composite powders prepared by spray pyrolysis. *Solid State Ion.* **2011**, *193*, 43–51. [[CrossRef](#)]
130. Li, M.; Hua, B.; Luo, J.-l.; Jiang, S.P.; Pu, J.; Chi, B.; Jian, L. Carbon-tolerant Ni-based cermet anodes modified by proton conducting yttrium- and ytterbium-doped barium cerates for direct methane solid oxide fuel cells. *J. Mater. Chem. A* **2015**, *3*, 21609–21617. [[CrossRef](#)]
131. Liu, Z.; Liu, B.; Ding, D.; Liu, M.; Chen, F.; Xia, C. Fabrication and modification of solid oxide fuel cell anodes via wet impregnation/infiltration technique. *J. Power Sources* **2013**, *237*, 243–259. [[CrossRef](#)]
132. Jiang, S.P. A review of wet impregnation—An alternative method for the fabrication of high performance and nano-structured electrodes of solid oxide fuel cells. *Mater. Sci. Eng. A* **2006**, *418*, 199–210. [[CrossRef](#)]
133. Lin, Y.; Zhan, Z.; Barnett, S.A. Improving the stability of direct-methane solid oxide fuel cells using anode barrier layers. *J. Power Sources* **2006**, *158*, 1313–1316. [[CrossRef](#)]
134. Zhan, Z.; Barnett, S.A. An octane-fueled solid oxide fuel cell. *Science* **2005**, *308*, 844–847. [[CrossRef](#)]
135. Li, T.; Wu, Z.; Li, K. Co-extrusion of electrolyte/anode functional layer/anode triple-layer ceramic hollow fibres for micro-tubular solid oxide fuel cells—electrochemical performance study. *J. Power Sources* **2015**, *273*, 999–1005. [[CrossRef](#)]
136. Zhu, H.; Colclasure, A.M.; Kee, R.J.; Lin, Y.; Barnett, S.A. Anode barrier layers for tubular solid-oxide fuel cells with methane fuel streams. *J. Power Sources* **2006**, *161*, 413–419. [[CrossRef](#)]
137. Zhang, P.; Yang, Z.; Jin, Y.; Liu, C.; Lei, Z.; Chen, F.; Peng, S. Progress report on the catalyst layers for hydrocarbon-fueled SOFCs. *Int. J. Hydrogen Energy* **2021**, *46*, 39369–39386. [[CrossRef](#)]
138. Steele, B.C.H.; Middleton, P.H.; Rudkin, R.A. Material science aspects of SOFC technology with special reference to anode development. *Solid State Ion.* **1990**, *40–41 Pt 1*, 388–393. [[CrossRef](#)]
139. Wang, K.; Ran, R.; Shao, Z. Methane-fueled IT-SOFCs with facile in situ inorganic templating synthesized mesoporous Sm<sub>0.2</sub>Ce<sub>0.8</sub>O<sub>1.9</sub> as catalytic layer. *J. Power Sources* **2007**, *170*, 251–258. [[CrossRef](#)]
140. Klein, J.M.; Georges, S.; Bultel, Y. SOFC fuelled by methane without coking: Optimization of electrochemical performance. *J. Appl. Electrochem.* **2010**, *40*, 943–954. [[CrossRef](#)]
141. Wang, W.; Zhou, W.; Ran, R.; Cai, R.; Shao, Z. Methane-fueled SOFC with traditional nickel-based anode by applying Ni/Al<sub>2</sub>O<sub>3</sub> as a dual-functional layer. *Electrochem. Commun.* **2009**, *11*, 194–197. [[CrossRef](#)]



142. Kan, H.; Lee, H. Sn-doped Ni/YSZ anode catalysts with enhanced carbon deposition resistance for an intermediate temperature SOFC. *Appl. Catal. B Environ.* **2010**, *97*, 108–114. [[CrossRef](#)]
143. Park, Y.M.; Kim, H. An additional layer in an anode support for internal reforming of methane for solid oxide fuel cells. *Int. J. Hydrogen Energy* **2014**, *39*, 16513–16523. [[CrossRef](#)]
144. Vernoux, P.; Guindet, J.; Kleitz, M. Gradual Internal Methane Reforming in Intermediate-Temperature Solid-Oxide Fuel Cells. *J. Electrochem. Soc.* **1998**, *145*, 3487–3492. [[CrossRef](#)]
145. Georges, S.; Parrour, G.; Henault, M.; Fouletier, J. Gradual internal reforming of methane: A demonstration. *Solid State Ion.* **2006**, *177*, 2109–2112. [[CrossRef](#)]
146. Nobrega, S.D.; Gelin, P.; Georges, S.; Steil, M.C.; Augusto, B.L.; Noronha, F.B.; Fonseca, F.C. A Fuel-Flexible Solid Oxide Fuel Cell Operating in Gradual Internal Reforming. *J. Electrochem. Soc.* **2014**, *161*, F354–F359. [[CrossRef](#)]
147. He, H.; Vohs, J.M.; Gorte, R.J. Carbonaceous deposits in direct utilization hydrocarbon SOFC anode. *J. Power Sources* **2005**, *144*, 135–140. [[CrossRef](#)]
148. Kim, T.; Liu, G.; Boaro, M.; Lee, S.I.; Vohs, J.M.; Gorte, R.J.; Al-Madhi, O.H.; Dabbousi, B.O. A study of carbon formation and prevention in hydrocarbon-fueled SOFC. *J. Power Sources* **2006**, *155*, 231–238. [[CrossRef](#)]
149. Kishimoto, H.; Horita, T.; Yamaji, K.; Xiong, Y.; Sakai, N.; Brito, M.E.; Yokokawa, H. Feasibility of n-Dodecane Fuel for Solid Oxide Fuel Cell with Ni-ScSZ Anode. *J. Electrochem. Soc.* **2005**, *152*, A532–A538. [[CrossRef](#)]
150. Iida, T.; Kawano, M.; Matsui, T.; Kikuchi, R.; Eguchi, K. Internal Reforming of SOFCs: Carbon Deposition on Fuel Electrode and Subsequent Deterioration of Cell. *J. Electrochem. Soc.* **2007**, *154*, B234–B241. [[CrossRef](#)]
151. Ahmed, K.; Föger, K. Fuel Processing for High-Temperature High-Efficiency Fuel Cells. *Ind. Eng. Chem. Res.* **2010**, *49*, 7239–7256. [[CrossRef](#)]
152. Park, K.; Lee, S.; Bae, G.; Bae, J. Performance analysis of Cu, Sn and Rh impregnated NiO/CGO91 anode for butane internal reforming SOFC at intermediate temperature. *Renew. Energy* **2015**, *83*, 483–490. [[CrossRef](#)]
153. Sammes, N.M.; Boersma, R.J.; Tompsett, G.A. Micro-SOFC system using butane fuel. *Solid State Ion.* **2000**, *135*, 487–491. [[CrossRef](#)]
154. Schädel, B.T.; Duisberg, M.; Deutschmann, O. Steam reforming of methane, ethane, propane, butane, and natural gas over a rhodium-based catalyst. *Catal. Today* **2009**, *142*, 42–51. [[CrossRef](#)]
155. Sun, C.; Xie, Z.; Xia, C.; Li, H.; Chen, L. Investigations of mesoporous CeO<sub>2</sub>-Ru as a reforming catalyst layer for solid oxide fuel cells. *Electrochem. Commun.* **2006**, *8*, 833–838. [[CrossRef](#)]
156. Liu, M.; Choi, Y.; Yang, L.; Blinn, K.; Qin, W.; Liu, P.; Liu, M. Direct octane fuel cells: A promising power for transportation. *Nano Energy* **2012**, *1*, 448–455. [[CrossRef](#)]
157. Ding, D.; Liu, Z.; Li, L.; Xia, C. An octane-fueled low temperature solid oxide fuel cell with Ru-free anodes. *Electrochem. Commun.* **2008**, *10*, 1295–1298. [[CrossRef](#)]
158. Zhan, Z.; Barnett, S.A. Operation of ceria-electrolyte solid oxide fuel cells on iso-octane–air fuel mixtures. *J. Power Sources* **2006**, *157*, 422–429. [[CrossRef](#)]
159. Zhan, Z.; Liu, J.; Barnett, S.A. Operation of anode-supported solid oxide fuel cells on propane–air fuel mixtures. *Appl. Catal. A Gen.* **2004**, *262*, 255–259. [[CrossRef](#)]
160. Zhan, Z.; Barnett, S. Use of a catalyst layer for propane partial oxidation in solid oxide fuel cells. *Solid State Ion.* **2005**, *176*, 871–879. [[CrossRef](#)]
161. Zhan, Z.; Barnett, S.A. Solid oxide fuel cells operated by internal partial oxidation reforming of iso-octane. *J. Power Sources* **2006**, *155*, 353–357. [[CrossRef](#)]
162. Murray, E.P.; Harris, S.J.; Liu, J.; Barnett, S.A. Direct Solid Oxide Fuel Cell Operation Using Isooctane. *Electrochem. Solid-State Lett.* **2006**, *9*, A292–A294. [[CrossRef](#)]
163. Yang, L.; Choi, Y.; Qin, W.; Chen, H.; Blinn, K.; Liu, M.; Liu, P.; Bai, J.; Tyson, T.A.; Liu, M. Promotion of water-mediated carbon removal by nanostructured barium oxide/nickel interfaces in solid oxide fuel cells. *Nat. Commun.* **2011**, *2*, 357. [[CrossRef](#)] [[PubMed](#)]
164. Shin, T.H.; Hagiwara, H.; Ida, S.; Ishihara, T. RuO<sub>2</sub> nanoparticle-modified (Ce,Mn,Fe)O<sub>2</sub>/(La,Sr) (Fe,Mn)O<sub>3</sub> composite oxide as an active anode for direct hydrocarbon type solid oxide fuel cells. *J. Power Sources* **2015**, *289*, 138–145. [[CrossRef](#)]
165. McIntosh, S.; Vohs, J.M.; Gorte, R.J. Role of Hydrocarbon Deposits in the Enhanced Performance of Direct-Oxidation SOFCs. *J. Electrochem. Soc.* **2003**, *150*, A470–A476. [[CrossRef](#)]
166. Gorte, R.J.; Park, S.; Vohs, J.M.; Wang, C. Anodes for Direct Oxidation of Dry Hydrocarbons in a Solid-Oxide Fuel Cell. *Adv. Mater.* **2000**, *12*, 1465–1469. [[CrossRef](#)]
167. Lu, C.; Worrell, W.L.; Gorte, R.J.; Vohs, J.M. SOFCs for Direct Oxidation of Hydrocarbon Fuels with Samaria-Doped Ceria Electrolyte. *J. Electrochem. Soc.* **2003**, *150*, A354–A358. [[CrossRef](#)]
168. Shao, Z.; Haile, S.M. A high-performance cathode for the next generation of solid-oxide fuel cells. *Nature* **2004**, *431*, 170–173. [[CrossRef](#)]
169. Lu, C.; An, S.; Worrell, W.L.; Vohs, J.M.; Gorte, R.J. Development of intermediate-temperature solid oxide fuel cells for direct utilization of hydrocarbon fuels. *Solid State Ion.* **2004**, *175*, 47–50. [[CrossRef](#)]

170. An, S.; Lu, C.; Worrell, W.L.; Gorte, R.J.; Vohs, J.M. Characterization of Cu–CeO<sub>2</sub> direct hydrocarbon anodes in a solid oxide fuel cell with lanthanum gallate electrolyte. *Solid State Ion.* **2004**, *175*, 135–138. [[CrossRef](#)]
171. Kaur, G.; Basu, S. Performance studies of copper–iron/ceria–yttria stabilized zirconia anode for electro-oxidation of butane in solid oxide fuel cells. *J. Power Sources* **2013**, *241*, 783–790. [[CrossRef](#)]
172. Dogdibegovic, E.; Fukuyama, Y.; Tucker, M.C. Ethanol internal reforming in solid oxide fuel cells: A path toward high performance metal-supported cells for vehicular applications. *J. Power Sources* **2020**, *449*, 227598. [[CrossRef](#)]
173. Ramadhani, F.; Hussain, M.A.; Mokhlis, H.; Hajimolana, S. Optimization strategies for Solid Oxide Fuel Cell (SOFC) application: A literature survey. *Renew. Sustain. Energy Rev.* **2017**, *76*, 460–484. [[CrossRef](#)]
174. Zhang, W.; Hu, Y.H. How stable is LiNi<sub>0.8</sub>Co<sub>0.15</sub>Al<sub>0.05</sub>O<sub>2</sub> under high-temperature hydrocarbon ceramic fuel cell conditions? *Ceram. Int.* **2023**, *49*, 3049–3057. [[CrossRef](#)]
175. Wang, W.; Qu, J.; Julião, P.S.B.; Shao, Z. Recent Advances in the Development of Anode Materials for Solid Oxide Fuel Cells Utilizing Liquid Oxygenated Hydrocarbon Fuels: A Mini Review. *Energy Technol.* **2019**, *7*, 33–44. [[CrossRef](#)]
176. Rabuni, M.F.; Li, T.; Punmeechao, P.; Li, K. Electrode design for direct-methane micro-tubular solid oxide fuel cell (MT-SOFC). *J. Power Sources* **2018**, *384*, 287–294. [[CrossRef](#)]
177. Tao, S.; Irvine, J.T.S. A redox-stable efficient anode for solid-oxide fuel cells. *Nat. Mater.* **2003**, *2*, 320–323. [[CrossRef](#)]
178. Gorte, R.J.; Vohs, J.M.; McIntosh, S. Recent developments on anodes for direct fuel utilization in SOFC. *Solid State Ion.* **2004**, *175*, 1–6. [[CrossRef](#)]
179. Cowin, P.I.; Petit, C.T.G.; Lan, R.; Irvine, J.T.S.; Tao, S. Recent Progress in the Development of Anode Materials for Solid Oxide Fuel Cells. *Adv. Energy Mater.* **2011**, *1*, 314–332. [[CrossRef](#)]
180. Zhu, W.Z.; Deevi, S.C. A review on the status of anode materials for solid oxide fuel cells. *Mat Sci Eng A-Struct* **2003**, *362*, 228–239. [[CrossRef](#)]
181. Mahato, N.; Banerjee, A.; Gupta, A.; Omar, S.; Balani, K. Progress in material selection for solid oxide fuel cell technology: A review. *Prog. Mater. Sci.* **2015**, *72*, 141–337. [[CrossRef](#)]
182. Li, T.; Rabuni, M.F.; Hartley, U.W.; Li, K. Chapter 9—Advanced ceramic membrane design for gas separation and energy application. In *60 Years of the Loeb-Sourirajan Membrane*; Tseng, H.-H., Lau, W.J., Al-Ghouti, M.A., An, L., Eds.; Elsevier: Amsterdam, The Netherlands, 2022; pp. 239–268.
183. Huang, K.; Tichy, R.S.; Goodenough, J.B. Superior Perovskite Oxide-Ion Conductor; Strontium- and Magnesium-Doped LaGaO<sub>3</sub>: I, Phase Relationships and Electrical Properties. *J. Am. Ceram. Soc.* **1998**, *81*, 2565–2575. [[CrossRef](#)]
184. Ishihara, T.; Matsuda, H.; Takita, Y. Doped LaGaO<sub>3</sub> Perovskite Type Oxide as a New Oxide Ionic Conductor. *J. Am. Chem. Soc.* **1994**, *116*, 3801–3803. [[CrossRef](#)]
185. Nagata, A.; Nishimoto, A. Low-temperature operation of thin film solid oxide fuel cells prepared by RF magnetron sputtering. *Electron. Commun. Jpn.* **2009**, *92*, 50–57. [[CrossRef](#)]
186. Li, T.; Wu, Z.; Li, K. Single-step fabrication and characterisations of triple-layer ceramic hollow fibres for micro-tubular solid oxide fuel cells (SOFCs). *J. Membr. Sci.* **2014**, *449*, 1–8. [[CrossRef](#)]
187. Kendall, K.; Palin, M. A small solid oxide fuel cell demonstrator for microelectronic applications. *J. Power Sources* **1998**, *71*, 268–270. [[CrossRef](#)]
188. Jamil, S.M.; Othman, M.H.D.; Rahman, M.A.; Jaafar, J.; Ismail, A.F.; Li, K. Recent fabrication techniques for micro-tubular solid oxide fuel cell support: A review. *J. Eur. Ceram. Soc.* **2015**, *35*, 1–22. [[CrossRef](#)]
189. Lee, M.; Wu, Z.; Wang, B.; Li, K. Micro-structured alumina multi-channel capillary tubes and monoliths. *J. Membr. Sci.* **2015**, *489*, 64–72. [[CrossRef](#)]
190. Li, T.; Rabuni, M.F.; Kleiminger, L.; Wang, B.; Kelsall, G.H.; Hartley, U.W.; Li, K. A highly-robust solid oxide fuel cell (SOFC): Simultaneous greenhouse gas treatment and clean energy generation. *Energy Environ. Sci.* **2016**, *9*, 3682–3686. [[CrossRef](#)]
191. Li, T.; Heenan, T.M.M.; Rabuni, M.F.; Wang, B.; Farandos, N.M.; Kelsall, G.H.; Matras, D.; Tan, C.; Lu, X.; Jacques, S.D.M.; et al. Design of next-generation ceramic fuel cells and real-time characterization with synchrotron X-ray diffraction computed tomography. *Nat. Commun.* **2019**, *10*, 1497. [[CrossRef](#)]
192. Othman, M.H.D.; Droushiotis, N.; Wu, Z.; Kelsall, G.; Li, K. Dual-layer hollow fibres with different anode structures for micro-tubular solid oxide fuel cells. *J. Power Sources* **2012**, *205*, 272–280. [[CrossRef](#)]
193. Li, T.; Wu, Z.; Li, K. A dual-structured anode/Ni-mesh current collector hollow fibre for micro-tubular solid oxide fuel cells (SOFCs). *J. Power Sources* **2014**, *251*, 145–151. [[CrossRef](#)]
194. Othman, M.H.D. *High Performance Micro-Tubular Solid Oxide Fuel Cell*; Imperial College London: London, UK, 2011.
195. Othman, M.H.D.; Droushiotis, N.; Wu, Z.; Kanawka, K.; Kelsall, G.; Li, K. Electrolyte thickness control and its effect on electrolyte/anode dual-layer hollow fibres for micro-tubular solid oxide fuel cells. *J. Membr. Sci.* **2010**, *365*, 382–388. [[CrossRef](#)]
196. Othman, M.H.D.; Droushiotis, N.; Wu, Z.; Kelsall, G.; Li, K. High-Performance, Anode-Supported, Microtubular SOFC Prepared from Single-Step-Fabricated, Dual-Layer Hollow Fibers. *Adv. Mater.* **2011**, *23*, 2480–2483. [[CrossRef](#)]
197. Li, T.; Wu, Z.; Li, K. High-efficiency, nickel-ceramic composite anode current collector for micro-tubular solid oxide fuel cells. *J. Power Sources* **2015**, *280*, 446–452. [[CrossRef](#)]
198. Lee, M.; Wang, B.; Li, K. New designs of ceramic hollow fibres toward broadened applications. *J. Membr. Sci.* **2016**, *503*, 48–58. [[CrossRef](#)]

199. Lu, X.; Li, T.; Bertei, A.; Cho, J.I.S.; Heenan, T.M.M.; Rabuni, M.F.; Li, K.; Brett, D.J.L.; Shearing, P.R. The application of hierarchical structures in energy devices: New insights into the design of solid oxide fuel cells with enhanced mass transport. *Energy Environ. Sci.* **2018**, *11*, 2390–2403. [[CrossRef](#)]
200. Rabuni, M.F.; Vatcharasuwan, N.; Li, T.; Li, K. High performance micro-monolithic reversible solid oxide electrochemical reactor. *J. Power Sources* **2020**, *458*, 228026. [[CrossRef](#)]

**Disclaimer/Publisher’s Note:** The statements, opinions and data contained in all publications are solely those of the individual author(s) and contributor(s) and not of MDPI and/or the editor(s). MDPI and/or the editor(s) disclaim responsibility for any injury to people or property resulting from any ideas, methods, instructions or products referred to in the content.